Neuroimaging Findings of Organic Acidemias and Aminoacidopathies

Reddy, Nihaal; Calloni, Sonia F; Vernon, Hilary J; Boltshauser, Eugen; Huisman, Thierry A G M; Soares, Bruno P

Abstract: Although individual cases of inherited metabolic disorders are rare, overall they account for a substantial number of disorders affecting the central nervous system. Organic acidemias and aminoacidopathies include a variety of inborn errors of metabolism that are caused by defects in the intermediary metabolic pathways of carbohydrates, amino acids, and fatty acid oxidation. These defects can lead to the abnormal accumulation of organic acids and amino acids in multiple organs, including the brain. Early diagnosis is mandatory to initiate therapy and prevent permanent long-term neurologic impairments or death. Neuroimaging findings can be nonspecific, and metabolism- and genetics-based laboratory investigations are needed to confirm the diagnosis. However, neuroimaging has a key role in guiding the diagnostic workup. The findings at conventional and advanced magnetic resonance imaging may suggest the correct diagnosis, help narrow the differential diagnosis, and consequently facilitate early initiation of targeted metabolism- and genetics-based laboratory investigations and treatment. Neuroimaging may be especially helpful for distinguishing organic acidemias and aminoacidopathies from other more common diseases with similar manifestations, such as hypoxic-ischemic injury and neonatal sepsis. Therefore, it is important that radiologists, neuroradiologists, pediatric neuroradiologists, and clinicians are familiar with the neuroimaging findings of organic acidemias and aminoacidopathies. RSNA, 2018.

DOI: https://doi.org/10.1148/rg.2018170042

Neuroimaging Findings of Organic Acidemias and Aminoacidopathies[1]

Nihaal Reddy, MD
Sonia F. Calloni, MD
Hilary J. Vernon, MD, PhD
Eugen Boltshauser, MD
Thierry A. G. M. Huisman, MD
Bruno P. Soares, MD

Although individual cases of inherited metabolic disorders are rare, overall they account for a substantial number of disorders affecting the central nervous system. Organic acidemias and aminoacidopathies include a variety of inborn errors of metabolism that are caused by defects in the intermediary metabolic pathways of carbohydrates, amino acids, and fatty acid oxidation. These defects can lead to the abnormal accumulation of organic acids and amino acids in multiple organs, including the brain. Early diagnosis is mandatory to initiate therapy and prevent permanent long-term neurologic impairments or death. Neuroimaging findings can be nonspecific, and metabolism- and genetics-based laboratory investigations are needed to confirm the diagnosis. However, neuroimaging has a key role in guiding the diagnostic workup. The findings at conventional and advanced magnetic resonance imaging may suggest the correct diagnosis, help narrow the differential diagnosis, and consequently facilitate early initiation of targeted metabolism- and genetics-based laboratory investigations and treatment. Neuroimaging may be especially helpful for distinguishing organic acidemias and aminoacidopathies from other more common diseases with similar manifestations, such as hypoxic-ischemic injury and neonatal sepsis. Therefore, it is important that radiologists, neuroradiologists, pediatric neuroradiologists, and clinicians are familiar with the neuroimaging findings of organic acidemias and aminoacidopathies.

Abbreviations: ADC = apparent diffusion coefficient, CBSD = cystathionine β-synthase deficiency, CSF = cerebrospinal fluid, D2HGA = D-2-hydroxyglutaric aciduria, FLAIR = fluid-attenuated inversion recovery, GA1 = glutaric aciduria type 1, L2HGA = L-2-hydroxyglutaric aciduria, MCCD = 3-methylcrotonyl coenzyme A carboxylase deficiency, MSUD = maple syrup urine disease, MTHFRD = 5,10-methylenetetrahydrofolate reductase deficiency, NAA = *N*-acetylaspartate, OMIM = Online Mendelian Inheritance in Man, 3HBA = 3-hydroxybutyric aciduria, 3HMGD = 3-hydroxy-3-methylglutaryl coenzyme A lyase deficiency

RadioGraphics 2018; 38:912–931

https://doi.org/10.1148/rg.2018170042

Content Codes: MR NR PD

[1]From the Division of Pediatric Radiology and Pediatric Neuroradiology, Russell H. Morgan Department of Radiology and Radiological Science (N.R., S.F.C., T.A.G.M.H., B.P.S.), and McKusick-Nathans Institute of Genetic Medicine, Department of Pediatrics (H.J.V.), The Johns Hopkins University School of Medicine, Charlotte R. Bloomberg Children's Center Bldg, Sheikh Zayed Tower, Room 4174, 1800 Orleans St, Baltimore, MD 21287-0842; Università degli Studi di Milano, Postgraduation School in Radiodiagnostics, Milan, Italy (S.F.C.); Department of Neurogenetics, Kennedy Krieger Institute, Baltimore, Md (H.J.V.); and Department of Pediatric Neurology, University Children's Hospital of Zurich, Zurich, Switzerland (E.B.). Presented as an education exhibit at the 2016 RSNA Annual Meeting. Received March 8, 2017; revision requested June 12 and received August 7; accepted September 25. For this journal-based SA-CME activity, the authors, editor, and reviewers have disclosed no relevant relationships. **Address correspondence to** B.P.S. (e-mail: *bruno.soares@jhmi.edu*).

SA-CME LEARNING OBJECTIVES

After completing this journal-based SA-CME activity, participants will be able to:

- Discuss the importance of rendering a precise diagnosis of inborn errors of metabolism—organic acidemias and aminoacidopathies in particular.
- Identify the neuroimaging findings of pediatric organic acidemias and aminoacidopathies.
- Describe the important clinical, genetic, and prognostic factors of each entity related to organic acidemias and aminoacidopathies and thus better address these entities with clinicians and patients.

See www.rsna.org/education/search/RG.

Introduction

Although inborn errors of metabolism are rare diseases individually, collectively they account for a remarkable number of disorders of the pediatric central nervous system, with an aggregate incidence of one in 1000 newborns (1,2). The majority of inborn errors of metabolism in newborns and infants are organic acid and amino acid disorders. The accumulation of amino acids in the bloodstream and the urinary excretion of these acids are termed *acidemia* and *aciduria,* respectively. These disorders are also known

TEACHING POINTS

- Symptoms characteristically occur postnatally after an interval of apparent good health. A catabolic episode such as infection, refusal to feed, dehydration, or excessive protein or carbohydrate load can trigger the onset of symptoms and sudden neurologic deterioration.
- An increased frequency of intracranial hemorrhage—seen as subarachnoid, intra- or periventricular, cerebellar, and diffuse petechial lesions in the white matter—has been reported with isovaleric acidemia.
- The ^{1}H MR spectrum in Canavan disease is pathognomonic and shows a markedly increased NAA peak level in both mild and severe cases and during the neonatal period, with the remaining MR imaging findings usually being normal.
- With GA1, subdural hematomas can be seen in symptomatic and asymptomatic patients, even during the immediate postnatal period. These hematomas can occur, sometimes repeatedly, with minimal trauma, mimicking abusive head trauma. The hematomas are presumably related to the rupture of bridging veins in the presence of cerebral atrophy.
- With nonketotic hyperglycinemia, ^{1}H MR spectroscopy will reveal a striking increase in the glycine peak level at 3.55 ppm. Because the glycine peak cannot be distinguished from the normal myo-inositol peak on short-echo MR spectra, the elevation in glycine concentration might be best evaluated by using long-echo ^{1}H MR spectra.

as organic acidopathies and aminoacidopathies. Affected newborns are usually asymptomatic at birth; however, earlier clinical onset occurs in children who have more profound enzymatic defects. Overall, the age of affected individuals at disease onset ranges from a few hours to months after birth. A correct diagnosis and the institution of appropriate therapy are critical to improving the long-term neurologic outcome and preventing death. Neuroimaging has an important role in the diagnostic workup of children suspected of having inborn errors of metabolism. The findings may be diagnostic or help to narrow the differential diagnosis and guide further diagnostic examinations.

In this article, we review the neuroimaging findings of organic acidemias and aminoacidopathies, beginning with a summary of the clinical manifestations and diagnostic workup of these disorders. The Online Mendelian Inheritance in Man (OMIM) phenotype number for each described acidemia and aminoacidopathy, as listed in the OMIM catalog of genetic disorders, is provided for reference.

Clinical Manifestations of Organic Acidemias and Aminoacidopathies in Children

Clinical phenotypes, which include acute life-threatening metabolic decompensation or crisis disorders that occur during the neonatal period and episodic or chronic deterioration that occurs at a later age (Table 1), can be variable and largely asymptomatic (1). Symptoms characteristically occur postnatally after an interval of apparent good health. A catabolic episode such as infection, refusal to feed, dehydration, or excessive protein or carbohydrate load can trigger the onset of symptoms and sudden neurologic deterioration. Typical symptoms at presentation include irritability, feeding difficulty, uncoordinated sucking or swallowing, abnormal muscle tone, persistent and severe vomiting, and seizures (Table 2). Vomiting may be misinterpreted as a manifestion of hypertrophic pyloric stenosis. In severely affected children, disease progression may lead to coma, episodic apnea, and death. In other children, symptoms may partially resolve and then recur after days or weeks.

Clinical examination of children with organic acidemias and aminoacidopathies during their well state typically reveals nonspecific findings, with a few notable exceptions (1). Corneal clouding, cataract, optic nerve abnormalities, and macular or retinal pigmentary changes may be helpful in establishing a diagnosis. Hepatomegaly may be present. An unusual odor of the child's body, cerumen, or urine has been associated with several organic acidemias and other amino acid metabolism disorders.

Diagnostic Workup of Organic Acidemias and Aminoacidopathies in Children

Once a patient's history and clinical presentation suggest an organic acidemia or aminoacidopathy, the diagnostic workup and general supportive measures should be started simultaneously. Although many of these disorders ultimately can be detected with newborn screening, neuroimaging should not be delayed until laboratory results are available or known because it may yield early crucial clues to the diagnosis and lead to the initiation of treatment to prevent or limit irreversible injury. Laboratory analyses of blood, urine, and/or cerebrospinal fluid (CSF) also have an important diagnostic role. These evaluations should include quantitative assessment of plasma amino acid, urine organic acid, and plasma carnitine (free and total) levels, and identification and quantification of acylcarnitines in plasma or serum.

Other basic analyses, including measurements of the hematologic cell count and electrolyte, blood glucose, liver transaminase, ammonia, lactic acid, pyruvic acid, and blood gas (venous or arterial) levels, should be performed to determine the acid-base status and, if applicable, the cause of the abnormal status (respiratory or metabolic). In addition, the homocysteine concentration may reveal information about the cobalamin metabolism.

Table 1: Timing of Manifestion of Pediatric Organic Acidemias and Aminoacidopathies

Disease*	Neonatal Period	Early Infantile Period	Late Infantile Period	Juvenile Period
Propionic acidemia	++	+	+	+
MMA	++	+	-	-
Isovaleric acidemia	++	+	-	-
MCCD	-	++	++	-
Biotinidase deficiency	-	++	+	++
HSD	++	+	+	-
βKD	++	+	-	-
Canavan disease	-	++	-	-
GA1	-	++	++	-
L2HGA	-	-	++	+
D2HGA	++	++	-	-
5-Oxoprolinuria	++	++	-	-
3HBA	++	-	-	-
3HMGD	++	-	-	-
Phenylketonuria	++	-	-	-
TYRSN1	++	-	-	-
MSUD	++	-	+	-
NKH	++	-	-	-
CBSD	-	++	+	-
MTHFRD	-	++	+	+
SOD and MOCD	++	-	-	-

Note.—The organic acidemias and aminoacidopathies that are rare (+), common (++), or not present (or no information is available) (-) during the given periods are listed.
*βKD = β-ketothiolase deficiency, CBSD = cystathionine β-synthase deficiency, D2HGA = D-2-hydroxyglutaric aciduria, GA1 = glutaric aciduria type 1, HSD = holocarboxylase synthetase deficiency, L2HGA = L-2-hydroxyglutaric aciduria, MCCD = 3-methylcrotonyl coenzyme A carboxylase deficiency, MMA = methylmalonic acidemia, MOCD = molybdenum cofactor deficiency, MSUD = maple syrup urine disease, MTHFRD = 5,10-methylene-tetrahydrofolate reductase deficiency, NKH = nonketotic hyperglycinemia, SOD = sulfite oxidase deficiency, 3HBA = 3-hydroxybutyric aciduria, 3HMGD = 3-hydroxy-3-methylglutaryl coenzyme A lyase deficiency, TYRSN1 = tyrosinemia type 1.

Additional testing may include measurements of CSF and plasma glycine levels—which are elevated in persons with glycine encephalopathy—and measurements of the urine *S*-sulfocysteine concentration, which is elevated in individuals with sulfite oxidase deficiency or molybdenum cofactor deficiency. It is preferable to collect samples during an acute episode, when metabolic abnormalities are most pronounced. The storage of adequate amounts of plasma, urine, blood (on filter paper), and CSF is important, and all biologic data should be collected at the same time, if possible (2). Specific enzyme assays and/or molecular studies to identify specific gene mutations can be performed thereafter.

Neuroimaging of Organic Acidemias and Aminoacidopathies in Children

In newborns, head ultrasonography is a reliable first-line imaging modality that can be performed at the bedside for early detection of brain edema or altered white matter echogenicity, which can be suggestive of metabolic brain injury (3). Magnetic resonance (MR) imaging is the most sensitive and specific neuroimaging tool for detection and assessment of organic acidemias and aminoacidopathies (4). Moreover, the integration of advanced MR imaging techniques such as diffusion-weighted imaging, diffusion-tensor imaging, and hydrogen 1 (^{1}H) MR spectroscopy enables more accurate and reliable anatomic-functional diagnoses. Diffusion-weighted imaging depicts early parenchymal changes and enables characterization of different types of parenchymal edema—mainly cytotoxic (ie, with low apparent diffusion coefficient [ADC] values) and vasogenic (ie, with increased ADC values) edema (5). Diffusion-tensor imaging can be used to characterize the directionality of water motion by means of measurement of the full tensor of the diffusion. Qualitative and quantitative ^{1}H-MR spectroscopic examinations are powerful noninvasive tools that can be used to study various brain metabolites.

Table 2: Key Clinical Features of Pediatric Organic Acidemias and Aminoacidopathies

Clinical Feature	Diseases*
Acute deterioration	MMA, IVA, HSD, 5-oxoprolinuria, βKD, 3HMGD, GA1
Progressive deterioration	L2HGA, 3HBA, Canavan disease
Recurrent deterioration	PA, MMA, MSUD, IVA
Macrocephaly	Canavan disease, GA1, L2HGA, D2HGA
Hypertonia	MMA, IVA
Ischemic events	PA, SOD, MOCD, HSD, CBSD, MTHFRD, 3HMGD
Ophthalmoplegia	MMA, PA, D2HGA, biotidinase deficiency, GA1, Canavan disease
Lens dislocation	SOD, MOCD, CBSD
Sensorineural hearing loss	Biotidinase deficiency
Craniofacial dysmorphism	D2HGA, SOD, MOCD, 3HBA
Breathing abnormalities	NKH
Acute pancreatitis	PA, MMA, IVA, MSUD, CBSD
Skin involvement	PKU, biotidinase deficiency
Peculiar odor	PKU (musty), IVA (sweaty feet), HSD (cat urine), MSUD (sweet syrup)
Lactic acidosis with hypoglycemia	3HMGD
Ketotic hypoglycemia	βKD, IVA, PA, MMA

*βKD = β-ketothiolase deficiency, HSD = holocarboxylase synthetase deficiency, IVA = isovaleric acidemia, MMA = methylmalonic acidemia, MOCD = molybdenum cofactor deficiency, NKH = nonketotic hyperglycinemia, PA = propionic acidemia, PKU = phenylketonuria, SOD = sulfite oxidase deficiency.

Confirmation of age-appropriate peak levels, detection of abnormal peak levels of metabolites such as glycine and lactate, and loss of peak levels of substances such as creatine may help in identifying aminoacidopathies (6). Susceptibility-weighted imaging is a high-spatial-resolution three-dimensional gradient-echo MR imaging technique involving phase postprocessing that increases the conspicuity of blood products, nonheme iron, and calcifications in the brain (7). Analysis of susceptibility-weighted phase images facilitates differentiation between intracranial calcifications and blood products.

Organic Acidemias

Organic acidemias are an important group of autosomal recessive inborn errors of metabolism. These errors are caused by defects in the intermediary metabolic pathways of carbohydrates, amino acids, and fatty acid oxidation, leading to the accumulation of organic acids in tissues and the subsequent excretion of these acids in urine (8).

Propionic Acidemia: OMIM 606054

Propionic acidemia is an autosomal recessive disorder caused by a deficiency in propionyl coenzyme A carboxylase, a biotin-requiring enzyme that catalyzes the conversion of propionyl coenzyme A to methylmalonyl coenzyme A in the metabolic pathways of valine, isoleucine, methionine, threonine, and odd-chain fatty acids. Propionic acidemia has an estimated incidence of one in 100 000 to one in 150 000 individuals (9).

In up to 80% of affected children, propionic acidemia manifests within the first 3 months of life, with metabolic decompensation clinically characterized by vomiting, poor feeding, lethargy, and coma related to severe ketoacidosis, hyperammonemia, hyperglycinemia, and decreased serum carnitine concentration (10). Propionic acidemia is increasingly being detected at newborn screening before the onset of symptoms. Intermittent and chronic progressive forms of this disorder also exist.

The neuroimaging findings of propionic acidemia are nonspecific. In affected neonates, characteristic acute neuroimaging findings include acute brain swelling with diffuse signal intensity abnormality and decreased diffusion in the cerebral white matter (Fig 1) (12,13). The basal ganglia are reported to be normal during the neonatal period. In older patients with acute decompensation, a hyperintense signal at T2-weighted and fluid-attenuated inversion-recovery (FLAIR) MR imaging, as well as decreased diffusion, is typically seen in the basal ganglia—mainly the putamen and caudate nucleus—and less commonly seen in the substantia nigra and dentate nucleus (14). The cerebral and cerebellar cortices and the subcortical white matter also may show abnormal signal intensity and mild swelling. During the chronic stage, early abnormal (delayed) myelination and later cortical and white matter atrophy with signal intensity changes of the basal ganglia usually are seen. During the acute decompensation stage, ^{1}H MR spectroscopy may reveal a decreased *N*-acetylaspartate (NAA) level,

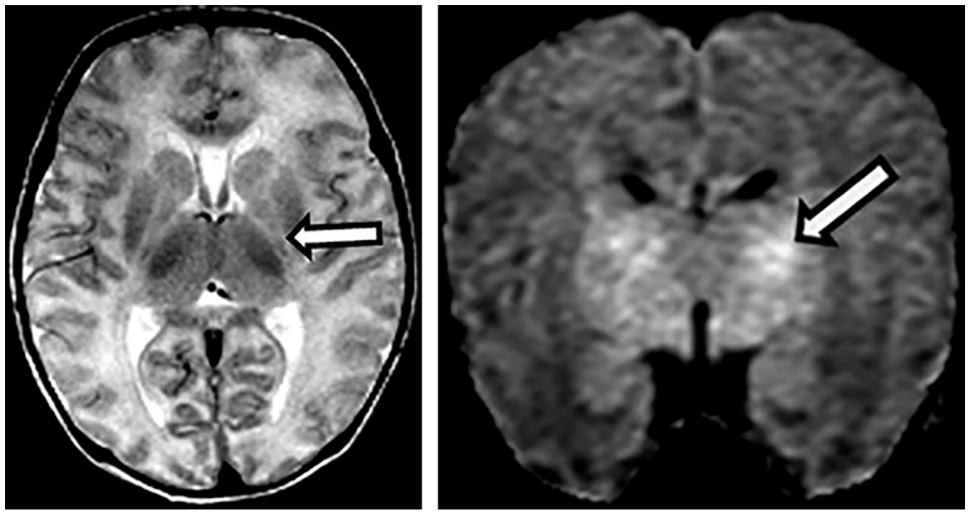

a. b.

Figure 1. Propionic acidemia in a 4-day-old neonate who presented with poor feeding, lethargy, hypothermia, and bradycardia, and had a markedly elevated blood ammonia level. **(a)** Axial T2-weighted MR image shows edema (arrow) surrounding the internal capsule and globi pallidi. **(b)** Coronal trace of diffusion-weighted image shows restricted diffusion (arrow) in the internal capsule and adjacent globi pallidi. (Reprinted, with permission, from reference 11.)

decreased glutamate and glutamine levels, and an increased lactate level (15,16). Finally, an increased frequency of intracranial hemorrhage has been reported in children with propionic acidemia (17).

Methylmalonic Acidemia: OMIM 251000

Methylmalonic acidemia is an autosomal recessive disease caused by a deficiency in methylmalonyl coenzyme A mutase, an adenosylcobalamin-requiring enzyme that catalyzes the conversion of L-methylmalonyl coenzyme A to succinyl coenzyme A in the metabolic pathways of valine, isoleucine, methionine, threonine, and odd-chain fatty acids (9). Methylmalonic acidemia can also be caused by defects in the adenosylcobalamin-cobalamin biosynthetic pathway. This disease has an estimated incidence of one in 50 000 individuals (9).

The clinical manifestations of methylmalonic acidemia are highly variable, depending on the severity of the enzyme defect, although failure to thrive, developmental delay, megaloblastic anemia, and neurologic dysfunction are common findings. Severely affected patients usually present during the neonatal period with poor feeding, dehydration, increasing lethargy, emesis, and hypotonia after a short asymptomatic period. They may also have ocular abnormalities such as retinopathy and nystagmus. Like propionic acidemia, methylmalonic acidemia is detectable with newborn screening and therefore may be detected presymptomatically. Hyperammonemia is a common feature of the severe early form of methylmalonic acidemia. Milder cases typically decompensate later during infancy or during childhood, with hypoglycemia, acidosis, seizures, and lethargy.

The neuroimaging findings of methylmalonic acidemia are nonspecific. Characteristic acute neuroimaging findings in neonates with methylmalonic acidemia include diffuse T2-hyperintense brain swelling with matching reduced diffusivity (Fig 2) (18). Follow-up MR imaging examinations performed at a later patient age may reveal cortical and white matter volume loss, with thinning of the corpus callosum, ventriculomegaly, signal intensity abnormalities of the periventricular and subcortical white matter, and basal ganglia calcifications. The basal ganglia calcifications are best seen on computed tomographic or susceptibility-weighted MR images (19). Bilateral infarctions of the globus pallidus may be seen at follow-up in approximately 50% of patients with methylmalonic acidemia (Fig 3). Bilateral infarctions usually are slightly asymmetric and mainly involve the posterior portion of the globus pallidus. Tiny lacunar infarctions in the pars reticulata of the substantia nigra also may be seen. ^{1}H MR spectroscopy may reveal a decreased NAA concentration and a lactate level peak during acute decompensation. However, MR imaging findings may also appear unremarkable (19).

Isovaleric Acidemia: OMIM 243500

Isovaleric acidemia is an autosomal recessive disorder caused by a deficiency in the mitochondrial enzyme isovaleryl coenzyme A dehydrogenase. This deficiency leads to the accumulation of several metabolites (20). Isovaleric acidemia

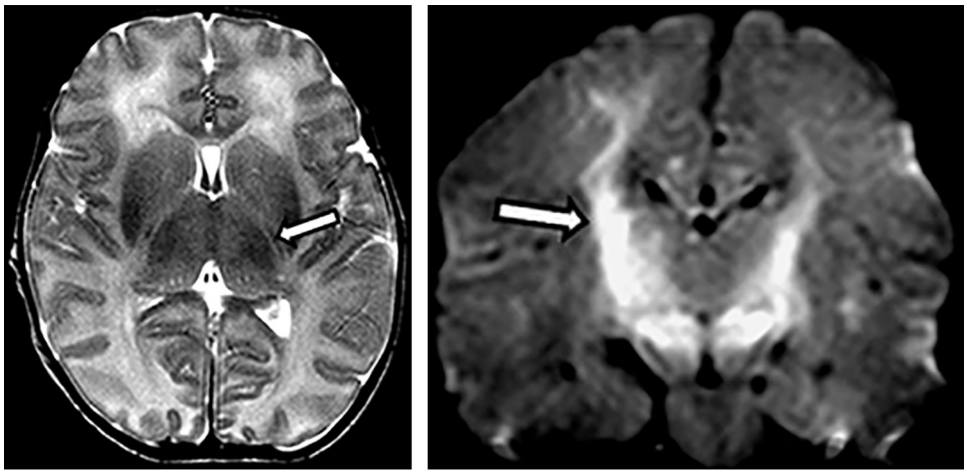

a. b.

Figure 2. Methylmalonic acidemia in a 6-day-old term newborn who was small for gestational age and found to have acute encephalopathy and hyperammonemia. **(a)** Axial T2-weighted MR image shows mildly increased signal intensity (arrow) surrounding the posterior limb of the internal capsule. **(b)** Coronal trace of diffusion-weighted image reveals restricted diffusion (arrow) in the corticospinal tracts as they course through the posterior limbs of the internal capsule to the brainstem. (Reprinted, with permission, from reference 11.)

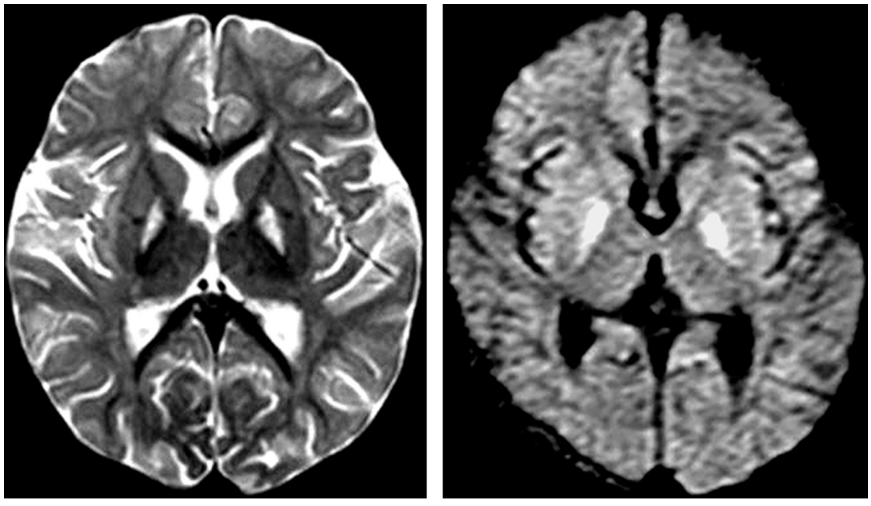

a. b.

Figure 3. Methylmalonic acidemia in an 18-month-old girl with acute metabolic crisis. **(a)** Axial T2-weighted MR image shows hyperintense signal in the globus pallidus bilaterally. **(b)** Matching axial trace of diffusion-weighted image obtained during the acute metabolic crisis reveals bilateral restricted diffusion in the globus pallidus. (Reprinted, with permission, from reference 4.)

has an estimated incidence of less than one in 200 000 individuals (21).

Isovaleric acidemia classically manifests with two phenotypes: early (ie, neonatal or infantile) metabolic crises that often lead to coma and a later-onset chronic intermittent course of disease that occurs during childhood (20). The acute form occurs in newborns and infants who are healthy at birth but later, during the first postnatal days, exhibit vomiting, feeding refusal, listlessness, dehydration, and lethargy. Seizures may occur, and the odor of sweaty feet is characteristic. Progression to coma and often death occur in nontreated infants. Children who survive typically develop a chronic intermittent form of isovaleric acidemia, which is characterized by episodes of vomiting, acidosis with ketonuria, lethargy that can progress to coma, and a characteristic odor that is triggered by an upper respiratory infection or ingestion of protein-rich food. Children with isovaleric acidemia who survive the metabolic crises intact often have normal cognitive development. However, mild cognitive impairment can occur.

The neuroimaging literature on isovaleric acidemia is limited, and the neuroimaging findings are nonspecific. A hypointense signal in the globus pallidus bilaterally at T1-weighted MR imaging, as well as a hyperintense signal in the globus pallidus bilaterally at T2-weighted and FLAIR MR imaging, has been reported (22). During the acute neonatal stage of this disease, T1-hypointense and T2-hyperintense signals in the supratentorial white matter may be seen without matching diffusion restriction (Fig 4a) (11). An increased frequency

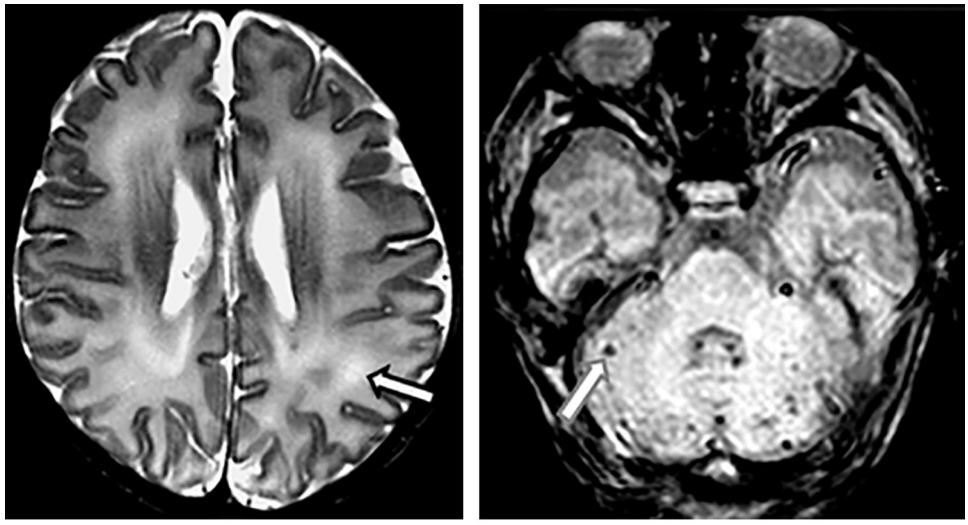

a. b.

Figure 4. Isovaleric acidemia in a 13-day-old newborn who presented with lethargy, jitteriness, and a sweaty smell. **(a)** Axial T2-weighted MR image shows mildly increased signal intensity (arrow) of the white matter. **(b)** Axial T2*-weighted MR image shows small multifocal hemorrhages (arrow) in the cerebellum. (Reprinted, with permission, from reference 11.)

of intracranial hemorrhage—seen as subarachnoid, intra- or periventricular, cerebellar, and diffuse petechial lesions in the white matter—has been reported with isovaleric acidemia (Fig 4b). Hemorrhage is best seen on susceptibility-weighted MR images and may result from various factors, such as brain edema due to the accumulation of abnormal organic acids, thrombocytopenia, and coagulopathy secondary to associated liver disease. This bleeding can also occur as a complication of anticoagulation therapy during hemofiltration to correct metabolic disturbances (17).

MCCD: OMIM 210200 and 210210

MCCD is an autosomal recessive disorder that affects the catabolic pathway of leucine. Biotin is a cofactor in this pathway. MCCD has an estimated incidence of one in 50 000 individuals (23).

Children with MCCD may present with a heterogeneous phenotype (24). Although many patients with MCCD remain asymptomatic, on rare occasion, affected patients become symptomatic during infancy or childhood, with episodes of vomiting, feeding difficulty, lethargy, hypotonia, hyperreflexia, hypoglycemia, metabolic acidosis, and ketosis in the context of a mild infection or other stress.

The neuroimaging literature on MCCD is limited; this is probably because of the typically milder clinical manifestations compared with those of other organic acidemias. Neuroimaging findings are nonspecific. During the acute phase, a hyperintense signal at T2-weighted and FLAIR MR imaging—with matching diffusion changes—may be seen bilaterally in the globi pallidi, thalami, cerebral peduncles, medulla oblongata, pons, inferior cerebellar peduncles, and periventricular white matter (25). Confluent and multifocal T2-hyperintense signal changes in the white matter may be the only neuroimaging findings (26). At follow-up, a rapid progression of gray and white matter atrophy associated with subdural hematomas is seen. ^{1}H MR spectroscopy may reveal elevated levels of lactate, branched-chain amino acids, glutamine, and glutamate (25). However, in mildly symptomatic or asymptomatic patients, neuroimaging findings are typically normal.

Multiple Carboxylase Deficiency

Multiple carboxylase deficiency refers to a group of biotin-responsive, autosomal recessive diseases with somewhat distinct but overlapping clinical manifestations. There are two main types of multiple carboxylase deficiency: biotinidase and holocarboxylase.

Biotinidase Deficiency: OMIM 253260.—Biotinidase deficiency is typically a later-onset form of multiple carboxylase deficiency caused by a deficiency in biotinidase activity that results in a lack of biotin recycling (27). The estimated incidence of biotinidase deficiency is one in 61 000 individuals. Because biotinidase deficiency can be detected with high sensitivity and specificity at newborn screening, it is often diagnosed and treated before the onset of clinical symptoms and radiologic abnormalities. Clinicians should be aware of the clinical manifestations of this deficiency when it is left untreated, given its highly treatable nature.

Children with biotinidase deficiency usually have lethargy, hypotonia, anorexia or vomiting, developmental delays, ataxia, and seizures—and can go into a state of coma—during the early to middle infancy period (27). Skin involvement is common and includes alopecia, rash, and mucocutaneous candidiasis. Hearing loss and optic atrophy are potential important long-term complications. Some patients present with motor weakness, spastic paresis, or loss of visual acuity during later childhood or adolescence.

The neuroimaging findings of biotinidase deficiency in children are nonspecific. Cerebral cortex and white matter atrophy with secondary enlargement of the ventricular system and extra-axial CSF spaces is the most common finding (27,28). Diffuse or patchy signal intensity abnormalities of the cerebral white matter (frontoparietal region in particular) and cerebellar white matter in association with restricted diffusion and subcortical cyst formation may be seen (28,29). In some children, a Leigh disease–like neuroimaging pattern with symmetric signal intensity abnormalities in the basal ganglia, medial thalami, dorsal midbrain, pons, and medulla may been seen (30). Signal intensity abnormality of the entire spinal cord at T2-weighted MR imaging, representing edema and/or demyelination and mimicking neuromyelitis optica, also may be seen (29–31). Finally, ^{1}H MR spectroscopy may reveal a lactate concentration peak and decreased NAA level (28). These findings may be entirely or partially reversible with early and adequate treatment (28).

Holocarboxylase Synthetase Deficiency: OMIM 253270.—Holocarboxylase synthetase deficiency is a life-threatening early-onset form of multiple carboxylase deficiency that is caused by a defect in holocarboxylase synthase activity (32). The estimated incidence is one in 200 000 individuals. This disease leads to a combined enzyme deficiency that causes an accumulation of several organic acids, including lactic, 3-hydroxyisovaleric, 3-hydroxypropionic, and methylcitric acids.

The clinical symptoms of holocarboxylase synthetase deficiency typically manifest within hours to a few weeks after birth and include irritability, lethargy, feeding problems, vomiting, tachypnea, and hypertonia or hypotonia. Without treatment, symptoms progress to intractable seizures and coma. Exfoliative dermatitis and hyperammonemia are commonly present.

The published literature on the neuroimaging findings of holocarboxylase synthetase deficiency is scant. Neuroimaging findings are nonspecific and typically include subependymal cysts, ventriculomegaly, and intraventricular hemorrhage that can be seen prenatally (33,34). However, some patients have normal neuroimaging findings (34).

β-Ketothiolase Deficiency: OMIM 203750

β-ketothiolase defiency is a rare organic acidemia that involves a common step in ketone body and isoleucine metabolism. It has an estimated incidence of one in 135 000 to one in 230 000 individuals (35).

The spectrum of clinical symptoms in children with β-ketothiolase defiency is wide. The majority of these children have intermittent episodes of ketoacidosis associated with vomiting, dyspnea, tachypnea, hypotonia, lethargy, and coma within the first 2 years of life (35). Children are typically well between the episodes.

The literature on the neuroimaging findings of β-ketothiolase defiency comprises only a few reports. A symmetric hypointense (at T1-weighted MR imaging) or hyperintense (at T2-weighted and FLAIR MR imaging) signal in the putamen (usually the posterior part) and/or globus pallidus bilaterally, with restricted diffusion, is the most common neuroimaging finding (36,37). In addition, a hyperintense signal of the dentate nuclei at T2-weighted and FLAIR MR imaging may be seen. ^{1}H MR spectroscopy may reveal a lactate level peak with an occasional increase in the choline concentration (38).

Canavan Disease: OMIM 271900

Canavan disease, also known as spongy degeneration of the brain, is an autosomal recessive disorder caused by a deficiency in aspartoacylase, which catalyzes the hydrolysis of NAA, leading to the accumulation of NAA (39). The estimated worldwide incidence is one in 100 000 individuals, with a higher incidence—one in 6400 to one in 13 500 individuals—in the Ashkenazi Jewish population. There is typically an increased concentration of NAA in the urine.

Canavan disease manifests in infantile and juvenile (late-onset) forms (39). Infantile Canavan disease is the most common, and affected infants present within the first 6 months of life with hypotonia, poor head control, poor eye contact, macrocephaly, irritability, and absence of early milestones. Later, these children may develop spasticity, opisthotonus, and decerebrate or decorticate posturing, and most of them die within the first 3 years of life. Children with late-onset Canavan disease may present with mild developmental delay, speech difficulties, and cognitive problems with neurologic regression.

The neuroimaging findings of Canavan disease are diagnostic. Macrocephaly is typically conspicuous at neuroimaging. In children with infantile-onset Canavan disease, conventional MR imaging

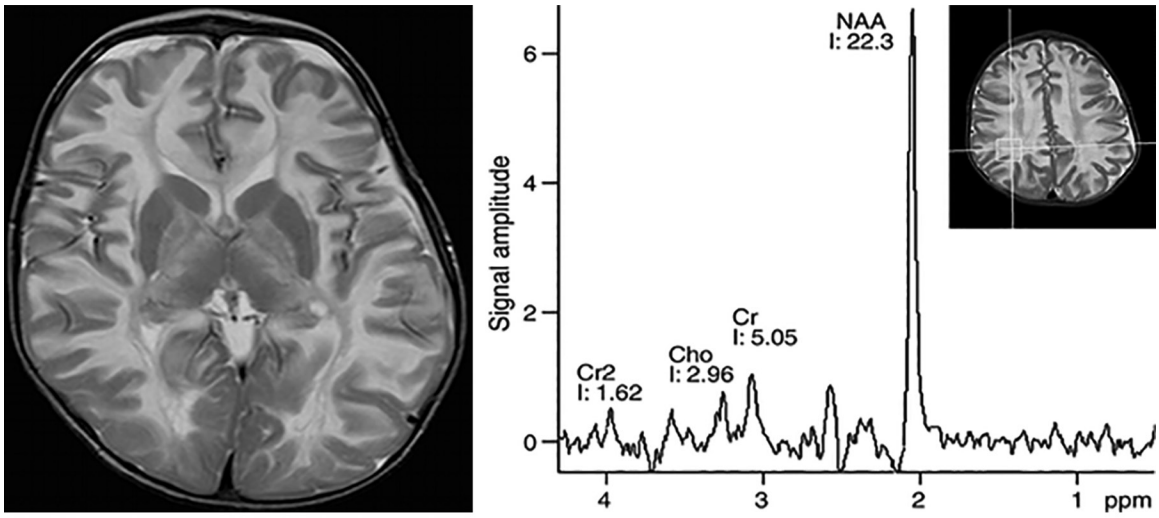

Figure 5. Canavan disease in a 6-month-old infant who presented with hypotonia, poor head control, absence of developmental milestones, and macrocephaly. **(a)** Axial T2-weighted MR image shows diffuse high signal intensity in the white matter, absence of myelination in the internal capsules, and high signal intensity in the globi pallidi and thalami. **(b)** Single-voxel ^{1}H MR spectrum sampling the right parietal white matter (as shown on the inset) shows a marked increase in the NAA level. *Cho* = choline, *Cr* and *Cr2* = creatine resonances.

sequences typically reveal diffuse symmetric areas of hypointense (on T1-weighted images) or hyperintense (on T2-weighted and FLAIR images) signal in the cerebral white matter, with predominant involvement of the subcortical white matter, which appears swollen, and partial sparing of the corpus callosum and internal capsule (Fig 5a) (40). During the course of the disease, the central periventricular white matter also becomes affected, and white matter atrophy with compensatory ventriculomegaly is typically seen at follow-up. In addition, the globi pallidi are almost always involved, the thalami are often affected, and the caudate nuclei and putamina are typically spared (Fig 5a). Brainstem tracts, cerebellar white matter, and dentate nuclei also may be affected.

The T2-weighted and FLAIR MR images obtained in children with a less severe course of the disease may show only a mild hyperintense signal of the arcuate fibers, striatum, dentate nuclei, and dorsal brainstem (41). Diffusion-weighted and diffusion-tensor images show restricted diffusion and low fractional anisotropy values in the affected white matter, which are most likely due to intramyelinic edema (42). The ^{1}H MR spectrum in Canavan disease is pathognomonic and shows a markedly increased NAA peak level (Fig 5b) in both mild and severe cases and during the neonatal period, with the remaining MR imaging findings usually being normal. The NAA peak level may decrease after gene therapy.

GA1: OMIM 231670

GA1 is an autosomal recessive disorder caused by a deficiency in glutaryl coenzyme A dehydrogenase activity. It has an estimated incidence of approximately one in 100 000 individuals (43). Glutaryl coenzyme A dehydrogenase is a key enzyme in the degradation pathway for lysine, hydroxylysine, and tryptophan. Deficient glutaryl coenzyme A dehydrogenase activity results in the accumulation of glutarate, glutarylcarnitine 3-hydroxyglutarate, and glutaconate in tissue, blood, CSF, urine, and multiple organs. Increased glutarate and 3-hydroxyglutarate levels may cause an imbalance in glutamatergic and γ-aminobutyric acid–mediated neurotransmission, and 3-hydroxyglutarate can cause excitotoxic cell damage mediated by the activation of *N*-methyl-D-aspartate receptors and result in striatal lesions (44). The diagnosis of GA1 is typically made on the basis of changes in organic acid levels and the acylcarnitine profile and confirmed with genetic analysis. Therapy—with carnitine supplementation and/or a low-lysine diet—should be started as soon as suspicion for GA1 is raised.

Children with GA1 typically present between the ages of 3 and 18 months with acute-onset dystonia and dyskinesia after an acute illness such as febrile viral infection of the upper airway (43). After an acute encephalopathic crisis, the affected child usually loses motor and language skills, and severe dystonia affects the long-term outcome. Intellectual functions may be relatively unaffected. Milder cases of GA1 without encephalopathic crises have been reported.

At MR imaging, symptomatic children have symmetric injury of the basal ganglia—the putamen and caudate nucleus in particular—whereas involvement of the globus pallidum is less common

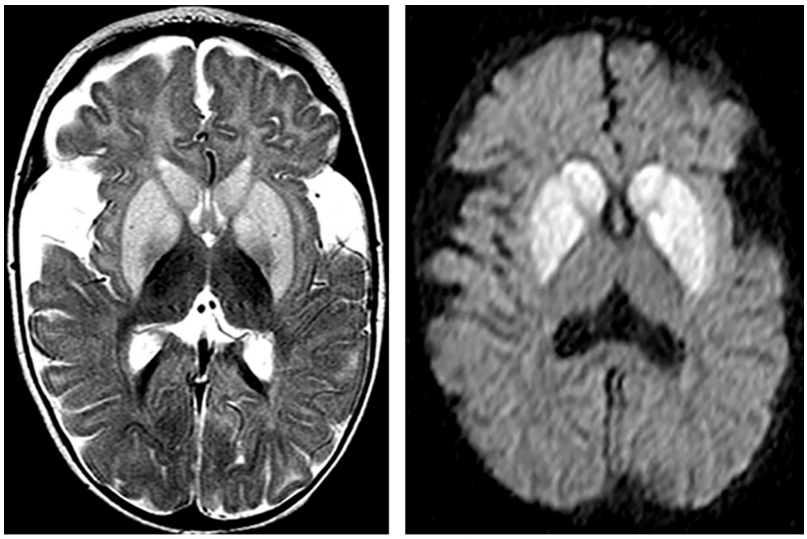

a. b.

Figure 6. GA1 in a 7-month-old infant with acute-onset dystonia. **(a)** Axial T2-weighted MR image shows swelling characterized by increased volume and high signal intensity in the bilateral striatum and enlarged sylvian fissures secondary to opercular hypoplasia. **(b)** Axial trace of diffusion-weighted image shows restricted diffusion in the striate nuclei during the acute phase of disease. (Reprinted, with permission, from reference 4.)

(45,46). The basal ganglia are swollen during the acute phase (Fig 6) and become atrophic as the disease progresses. Putaminal changes seen at MR imaging are reliable predictors of long-term movement disorders (45). In addition, abnormalities are often seen in the upper brainstem, with increased signal intensity of the substantia nigra, central tegmental tracts, tegmentum, dentate nuclei, and white matter at T2-weighted MR imaging. The white matter changes are usually patchy and scattered and are mainly seen as small foci of gliosis in subcortical regions. Bilateral but not necessarily symmetric enlargement of subarachnoid CSF spaces in the temporal fossa and, in particular, widening of the sylvian fissures due to opercular hypoplasia are characteristic of GA1 (Fig 7a, 7b).

With GA1, subdural hematomas can be seen in symptomatic and asymptomatic patients, even during the immediate postnatal period. These hematomas can occur, sometimes repeatedly, with minimal trauma, mimicking abusive head trauma. The hematomas are presumably related to the rupture of bridging veins in the presence of cerebral atrophy. Retinal hemorrhage also has been reported. Advanced neuroimaging techniques may help to facilitate the diagnostic workup. Restricted diffusion is usually seen in the basal ganglia and white matter during the acute metabolic crisis. ^{1}H MR spectroscopy may reveal a mild increase in the lactate level during the acute phase, whereas the NAA level is typically decreased during the subacute and chronic phases.

L2HGA: OMIM 236792

L2HGA is an autosomal recessive disease caused by mutations in *L2HGDH,* the mitochondrial enzyme gene, which cause the accumulation of L-2-hydroxyglutaric acid in urine, CSF, and plasma (47). The exact prevalence of L2HGA is unknown; about 150 cases have been published so far. An increased incidence of brain tumors such as medulloblastoma has been reported (48). The diagnosis of L2HGA is made on the basis of an increase in the urinary excretion of 2-hydroxyglutaric acid without any other organic acid abnormality.

Children with L2HGA typically present with developmental delay, hypotonia, ataxia, and seizures within the 1st year of life (49). Macrocephaly is mentioned in most reported cases in the literature, but it occurs in approximately half of the individuals with this disorder (50). The course of this disease is progressive, and affected children usually develop spasticity, extrapyramidal movement disorders, and behavioral problems and experience a progressive decline in previously acquired skills.

The neuroimaging findings of L2HGA are diagnostic and highly consistent. High signal intensity in the cerebral white matter, predominantly involving the frontal and subcortical regions, which may appear swollen and be multifocal initially, is typically seen on T2-weighted and FLAIR MR images (Fig 8a) (49,50). The white matter signal intensity abnormalities later become more confluent; however, the periventricular white matter, corpus callosum, posterior limb of the internal capsule, cerebellar white matter, and brainstem remain relatively spared. The dentate nuclei are consistently T2 hyperintense (Fig 8b); usually the basal ganglia also are involved and the thalami are spared (50). Cerebellar atrophy may occur. Diffusion-weighted and diffusion-tensor imaging results usually are unremarkable. ^{1}H MR spectroscopy may reveal a mild decrease in the NAA level and an increased myo-inositol level (51).

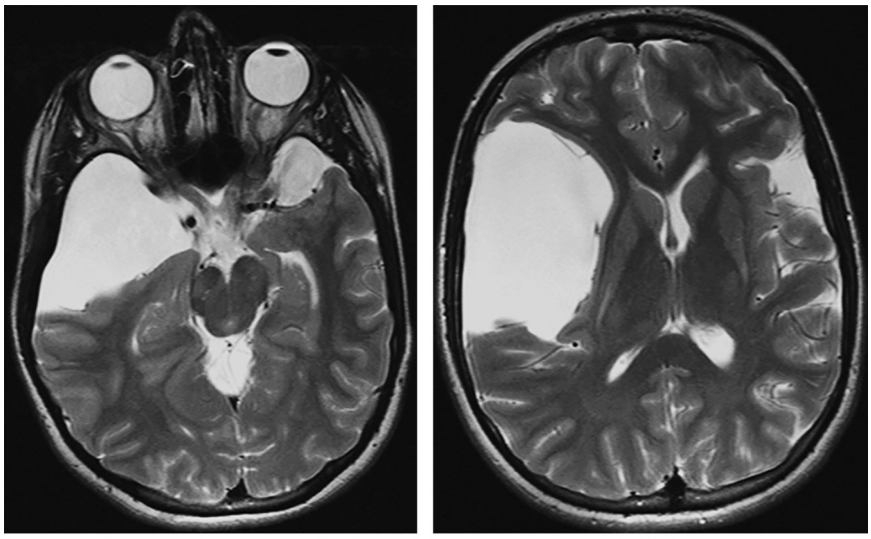

Figure 7. GA1 and mild dyskinetic movement disorder in an 18-year-old woman. Axial T2-weighted MR images show large asymmetric arachnoid cysts in the bilateral middle cranial fossae **(a)**, with superior extension to the sylvian fissure on the right **(b)**. In addition, bilateral high signal intensity and atrophy are seen in the dorsal putamina, consistent with prior injury.

a. **b.**

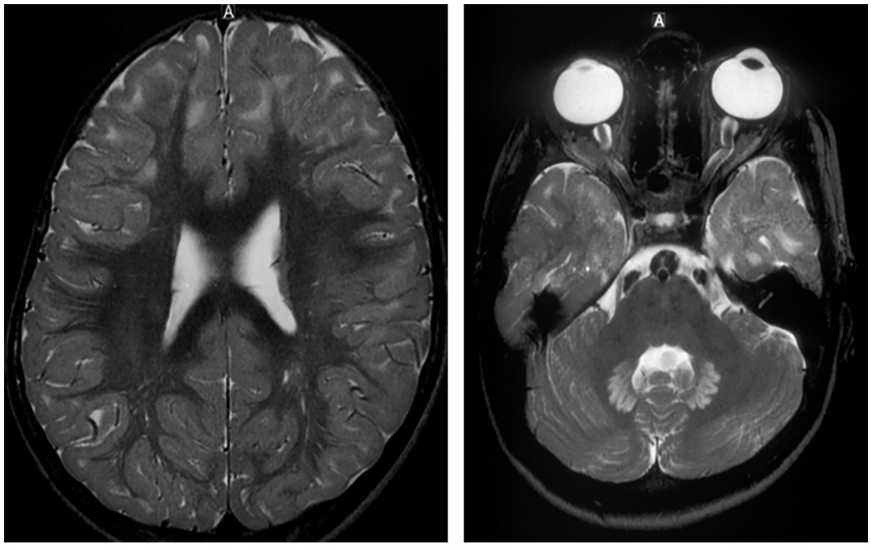

Figure 8. L2HGA in a 2-year-old boy with macrocephaly, ataxia, and hypotonia. **(a)** Axial T2-weighted MR image shows increased signal intensity in the subcortical white matter, with sparing of the central deep white matter and corticospinal tracts. **(b)** Axial T2-weighted MR image shows bilateral high signal intensity of the dentate nuclei.

a. **b.**

D2HGA: OMIM 600721 and 613657

D2HGA is a rare autosomal recessive disorder caused by a deficiency in the mitochondrial enzyme D-2-hydroxyglutarate dehydrogenase, which leads to the accumulation of D-2-hydroxyglutaric acid in urine, plasma, and CSF (52). The exact prevalence of D2HGA is unknown; about 80 cases have been published so far. Rarely, a combination of D2HGA and L2HGA occurs owing to *SLC25A1* mutations. The diagnosis is made on the basis of increased urinary excretion of 2-hydroxyglutaric acid. However, this finding does not enable differentiation between L2HGA and D2HGA.

D2HGA can manifest as a severe disorder with a neonatal or early-infantile onset or as a milder disorder with a later onset (53). The severe phenotype is characterized by marked hypotonia, developmental delay, seizures, vision loss, cardiomyopathy, and facial dysmorphic features. A subtype of this disorder, D2HGA type II, also involves cardiomyopathy as a key feature. The phenotype of the mild form is variable, with developmental delay and hypotonia being the most common findings.

In contrast to the characteristic MR imaging findings of L2HGA, the neuroimaging findings of severe D2HGA in infants are less consistent. These findings typically include nonspecific imaging features such as a delayed or simplified gyral pattern, delayed myelination, subependymal germinolytic cysts, mild ventriculomegaly with predominant involvement of the posterior horns of the lateral ventricles, and enlargement of the extra-axial CSF spaces with secondary subdural hemorrhage (Fig 9) (53,54). Follow-up images may show progression of gyral folding with development of

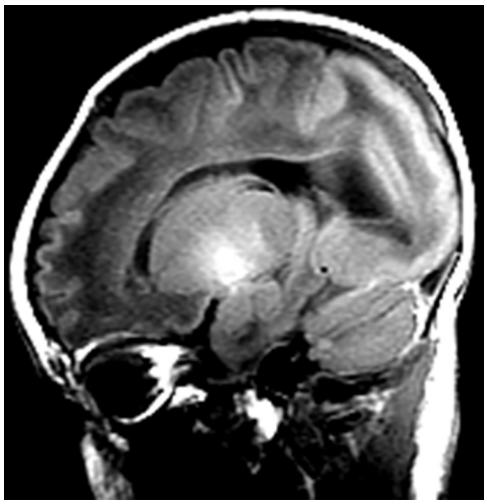

Figure 9. D2HGA in a 5-day-old boy. Sagittal T1-weighted MR image shows extensive parieto-occipital pachygyria and a subependymal cyst. (Reprinted, with permission, from reference 4.)

secondary and tertiary sulci. Myelination remains delayed, and patchy white matter signal intensity abnormalities may be seen. Multiple aneurysms of the cerebral arteries were found in one patient (55). In patients with mild D2HGA, germinolytic cysts and delayed myelination may be the only findings. Patients with combined D2HGA and L2HGA usually have neuroimaging findings similar to those in patients with severe D2HGA.

5-Oxoprolinuria: OMIM 260005

5-Oxoprolinuria, or pyroglutamic aciduria, is an autosomal recessive disorder that is caused by errors in the synthesis and degradation of glutathione and results in the massive urine excretion of 5-oxoproline (56). Fewer than 100 patients with this disease have been reported on so far.

The clinical manifestations of 5-oxoprolinuria may include metabolic acidosis, mental retardation, ataxia, spasticity, seizures, psychiatric disturbances, recurrent bacterial infections due to defective granulocyte function, and hemolytic anemia (56). The neuroimaging literature on 5-oxoprolinuria is based only on a few case reports that also include autopsy data. Neuroimaging findings may be normal or indicate cerebral atrophy over time (57,58).

3HBA: OMIM 236795

3HBA is probably an autosomal recessive valine metabolism disorder (59). Fewer than 15 cases have been reported to date. Children with 3HBA typically have hypotonia, seizures, failure to thrive, dehydration, episodes of ketoacidosis, lactic acidemia, and lethargy during the neonatal period (59). Dysmorphic facial features also may be seen.

The neuroimaging literature on 3HBA is based only on a few case reports. During the ketoacidotic episode, bilateral swelling and signal intensity abnormality of the putamina and caudate nucleus heads may be seen (60). In addition, single cases of cortical abnormalities such as lissencephaly and polymicrogyria, callosal dysgenesis, focal white matter signal intensity abnormality, ventriculomegaly, and cerebellar dysplasia have been reported (61,62).

3HMGD: OMIM 246450

3HMGD is an autosomal recessive organic aciduria caused by a deficiency in 3-hydroxy-3-methylglutaryl coenzyme A lyase, a key enzyme in ketogenesis and leucine metabolism (63). The estimated incidence is less than one in 100 000 individuals.

The majority of children with 3HMGD present during the neonatal period—after a short symptom-free interval—with hypotonia, lethargy, seizures, vomiting, and dehydration. They may also have severe hypoketotic hypoglycemia. Acute encephalopathic crises with metabolic acidosis and hypoglycemia may recur, usually owing to noneating or infection, and result in permanent and severe neurologic compromise.

Neuroimaging findings include diffuse mild or multifocal, more severe foci of white matter signal intensity abnormality that typically spare the corpus callosum, subcortical arcuate fibers, and cerebellar white matter (64,65). In addition, signal intensity abnormalities of the basal ganglia (head of the caudate nuclei and anterior part of the putamina), dentate nuclei, and brainstem tegmentum may be seen. ^{1}H MR spectroscopy can be diagnostic and reveal abnormal positive peaks at 1.3 and 2.4 ppm, which most likely represent 3-hydroxy-3-methylglutaryl coenzyme A lyase(64,65).

Aminoacidopathies

Aminoacidopathies are an important group of autosomal recessive inborn errors of metabolism. They are caused by the deficiency in an enzyme or transporter involved in amino acid metabolism (66).

Phenylketonuria: OMIM 261600

Phenylketonuria is an autosomal recessive disorder with an incidence of one in 10 000 people in the general population of white individuals. However, it is more common in Turkey, Scotland, Czech Republic, Slovakia, Arabic populations, and persons of Yemenite Jewish ancestry (one in 2500 to one in 5000 people) (67). Phenylketonuria is caused by mutations in the *PAH* gene, which result in high values of phenylalanine. The high phenylalanine values seem to be the cause of neurotoxicity.

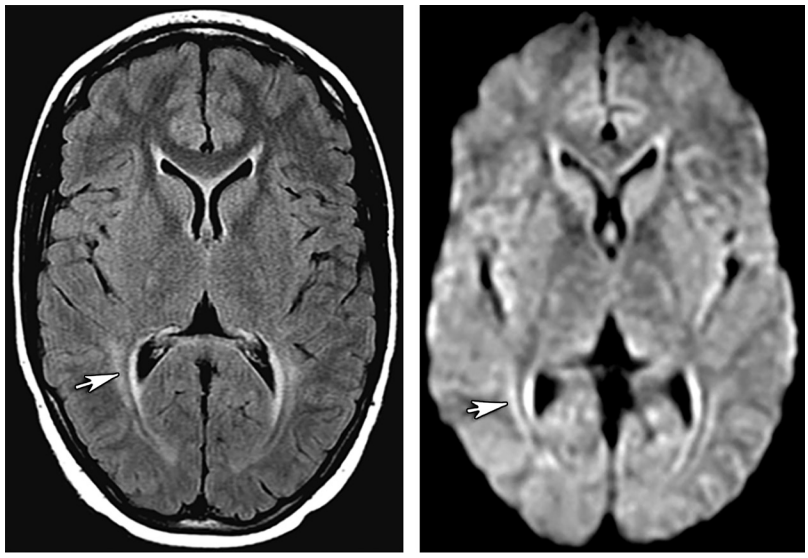

a. b.

Figure 10. Phenylketonuria in a 17-year-old girl. **(a)** Axial FLAIR MR image shows increased signal intensity (arrow) of the periventricular white matter. **(b)** Matching axial trace of diffusion-weighted image shows high signal intensity (arrow) of the periventricular white matter, representing restricted diffusion and intramyelinic edema. (Reprinted, with permission, from reference 4.)

In most patients, the diagnosis of phenylketonuria is made at routine newborn screening in asymptomatic neonates (68). Children who maintain goal levels of plasma phenylalanine by means of dietary restriction of phenylalanine intake typically have normal cognitive development. Nontreatment of classic phenylketonuria results in profound intellectual disability. Acute metabolic encephalopathy, a common feature of many organic acidurias and aminoacidopathies, does not occur with phenylketonuria. Children with phenylketonuria usually are healthy at birth and have normal early development, even if they are not treated. Over time, classically affected patients develop microcephaly, spasticity, tremor, and athetosis and will have seizures. Psychiatric and behavioral problems, including autistic behavior and attention deficit hyperactivity disorder, are common. Affected individuals may have lighter pigmentation, eczema, and a musty odor attributed to phenylacetic acid.

At neuroimaging, T2-weighted and FLAIR MR images may show a hyperintense signal in the periventricular white matter that may also affect the subcortical white matter. This high signal intensity probably reflects hypomyelination in nontreated patients and intramyelinic edema in early-treated patients—findings that are best depicted on diffusion-weighted and diffusion-tensor images (Fig 10) (69,70). White matter changes seem to be reversible with adherence to a strict low-phenylalanine diet. Patient age and quality of dietary control were shown to have independent cumulative effects on the outcome of patients with white matter alterations (71). Over time, ventriculomegaly and secondary atrophy may develop. ^{1}H MR spectroscopy may reveal a peak at 7.37 ppm, corresponding to phenylalanine.

Tyrosinemia Type 1: OMIM 276700

Tyrosinemia type 1 is an autosomal recessive disorder caused by a defect in fumarylacetoacetase; this enzyme has a key role in the pathway of degradation of tyrosine (72). As a result, toxic metabolites such as succinylacetone, maleylacetoacetate, and fumarylacetoacetate are formed and cause severe disruption of the intracellular metabolism of the liver and kidneys. Tyrosinemia type 1 has an incidence of approximately one in 100 000 individuals.

A characteristic manifestation of tyrosinemia type 1 is acute liver failure that occurs during the first weeks or months of life and results in coagulation abnormalities, hemorrhage, ascites, and cirrhosis, with the risk of hepatocellular carcinoma later. Renal tubular disorder with Fanconi syndrome (ie, excess excretion of glucose, bicarbonate, phosphates, uric acid, potassium, and/or amino acids)—not to be confused with Fanconi anemia—also is characteristic of this disease (72). Some affected patients develop neurologic symptoms with pain, weakness (acute ascending motor neuropathy), and autonomic changes such as arterial hypertension.

Data on the neuroimaging findings in children with tyrosinemia type 1 are scant. Brain MR images obtained in one child showed T2-hyperintense signal changes in the globus pallidus (73). In another reported case, diffusion-weighted images showed restricted diffusion in the centrum semiovale and corticospinal tracts (74).

MSUD: OMIM 248600

MSUD is an autosomal recessive defect in the catabolism of branched-chain amino acids (ie, leucine, isoleucine, and valine). It is caused by mutations in any of the components of the

mitochondrial branched-chain α-keto acid dehydrogenase complex (75).

In its classic form, MSUD manifests at the end of the 1st week of life, with severe neonatal encephalopathy, poor feeding, and vomiting. Dystonia (rhythmic boxing and cycling movements of the limbs), opisthotonic posturing, fluctuating ophthalmoplegia, and seizures follow (76). MSUD can be detected at newborn screening to facilitate presymptomatic initiation of therapy. Early detection is critical, as initiation of therapy within the first 5 days of life is associated with an improved neurodevelopmental outcome (77).

An odor similar to that of maple syrup or burnt sugar in the cerumen at 24–48 hours of life or in the urine during the latter part of the 1st week of life suggests a diagnosis of MSUD. The diagnosis can be confirmed by detection of increased values of branched-chain amino acids in blood or urine (76). However, some affected children present for medical attention later—at 5 months to 2 years of age—with episodes of neurologic decompensation characterized by ataxia, disorientation, and altered behavior. The crises associated with the intermittent form of MSUD are usually triggered by infection or high protein intake.

The neuroimaging findings of MSUD—the characteristic pattern of edema at diffusion-weighted imaging in particular—are diagnostic. Two types of brain edema can be seen with MSUD: intramyelinic edema and vasogenic edema. Intramyelinic edema is the intense form that affects the myelinated white matter (cerebellar white matter, dorsal brainstem, cerebral peduncles, posterior limb of the internal capsule, and perirolandic cerebral white matter), and the thalami and globi pallidi, both of which have a high density of myelinated fibers. Intramyelinic edema has the typical pattern of edema related to MSUD: high signal intensity on T2-weighted and diffusion-weighted MR images, low signal intensity on T1-weighted MR images, and decreased ADC and fractional anisotropy values (Fig 11) (78–81).

Intramyelinic edema is thought to be caused by energy failure that results in decreased sodium-potassium adenosine triphosphatase activity due to the accumulation of branched-chain keto acids. The accumulation of water molecules between the myelinic lamellae results in decompaction and splitting of the myelin layering. The resulting myelin instability and ongoing fiber destruction, as indicated by decreased fractional anisotropy values, can be detected at diffusion-tensor imaging (80,81). Delayed myelination and white matter atrophy are possible long-term sequelae. The intramyelinic edema may regress, but it frequently persists after initiation of therapy (80).

In addition to intramyelinic edema, a superimposed vasogenic edema involving the unmyelinated brain structures may be observed. This second type of edema is due to blood-brain barrier disruption that causes a global increase in water in the extracellular spaces and is present only during acute metabolic decompensation or crisis (80,81).

The ^{1}H MR spectroscopic findings of MSUD include a lactate level peak (ie, anaerobic glycolysis due to energy failure) and a peak at 0.9 ppm representing branched-chain amino acids and keto acids (78). These peaks may be absent in newborns who have undergone urgent dialysis and/or hemofiltration before MR imaging and/or ^{1}H MR spectroscopy.

Nonketotic Hyperglycinemia: OMIM 605899

Nonketotic hyperglycinemia, or glycine encephalopathy, is a rare autosomal recessive disorder that is caused by a defective glycine cleavage system. This disorder leads to the accumulation of large amounts of glycine in body fluids and tissues and subsequent central nervous system toxicity (82). The neurotoxicity of glycine seems to be related to excitatory and inhibitory neuronal effects on glycine and *N*-methyl-D-aspartate receptors in the telencephalon and brainstem–spinal cord complex, respectively, and a disturbance in myelin proteins (83). The incidence of nonketotic hyperglycinemia is estimated to be one to nine in 1 000 000 individuals.

The majority of patients with nonketotic hyperglycinemia present during the neonatal period. Newborns typically present during the first 2 days of life with progressive lethargy, hypotonia, and myoclonic jerks rapidly evolving into apnea, coma, and often death (82). Hiccups, which may have a prenatal onset, and abnormal ocular movements are additional symptoms. The majority of surviving infants have profound intellectual disabilities and intractable seizures. Neonatal electroencephalographic results are abnormal in at least 90% of cases and usually show a burst-suppression pattern. The diagnosis of nonketotic hyperglycinemia is established by an increase in CSF glycine concentration and an increased CSF glycine–to–plasma glycine ratio, with the CSF and plasma glycine concentrations simultaneously sampled.

The neonatal neuroimaging findings include structural and white matter abnormalities. Agenesis or dysgenesis of the corpus callosum is the most common structural abnormality related to nonketotic hyperglycinemia and, when associated with the clinical manifestations, is suggestive of the diagnosis (84). In addition, hypoplasia of the cerebellar vermis—the inferior part in particular—has been reported (84). The myelinated

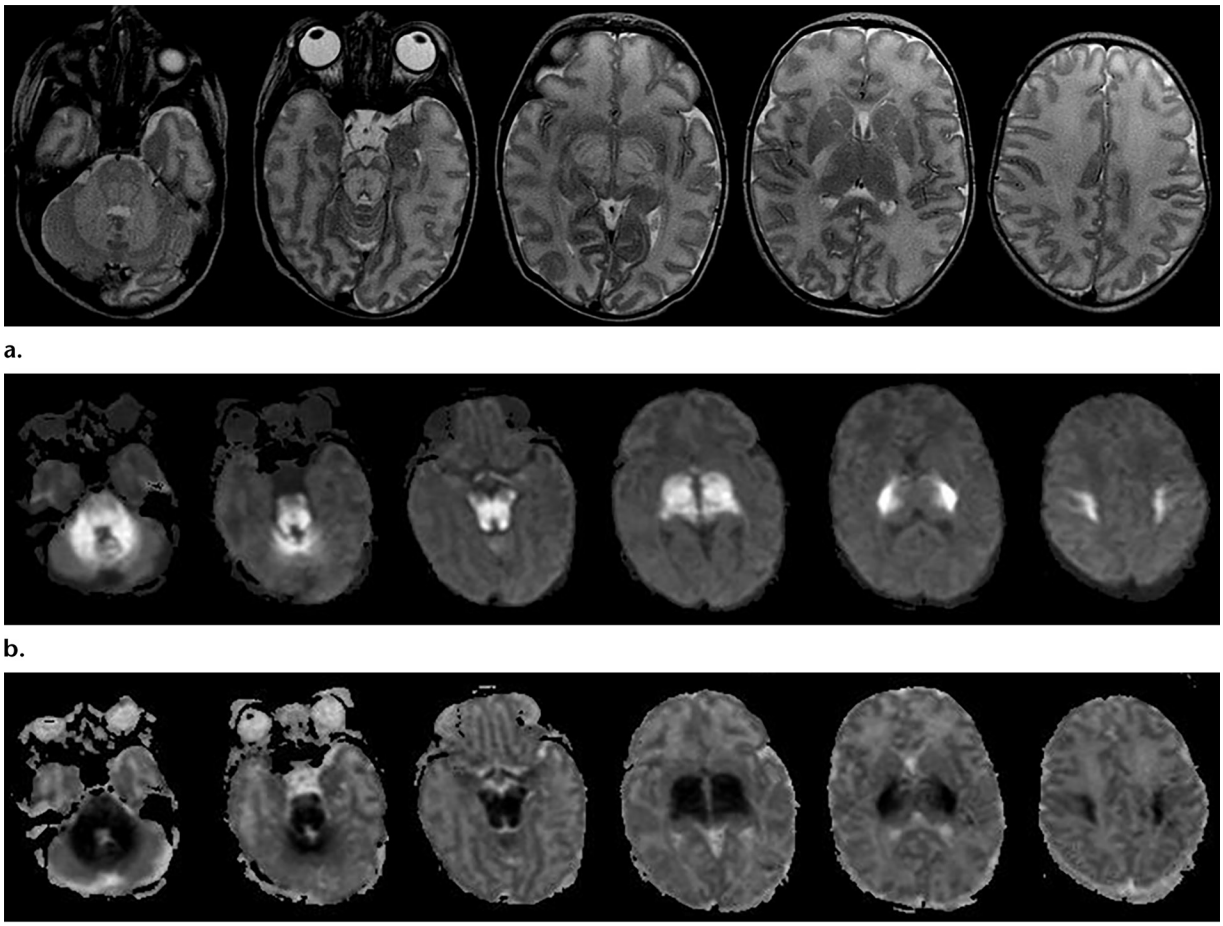

Figure 11. MSUD in a 10-day-old neonate with encephalopathy, poor feeding, vomiting, and rhythmic boxing and cycling movements of the limbs. **(a)** Axial T2-weighted MR images show hyperintense signal and swelling of the cerebellar white matter, dorsal pons, corticospinal tracts in the basis pontis, midbrain, posterior limb of the internal capsule, thalami, and central corona radiata. **(b, c)** Matching axial traces of diffusion-weighted images **(b)** and ADC maps **(c)** show high signal intensity and low ADC values, representing restricted diffusion, in the same regions of the brain. (Reprinted, with permission, from reference 11.)

white matter is affected and appears T2 hyperintense (Fig 12a), and the degree of involvement is best seen on diffusion-weighted images (84,85). Restricted diffusion in the myelinated white matter tracts is indicated by matching low ADC values and is due to myelin vacuoles secondary to the splitting of the myelin sheets (Fig 12b) (85).

Sequential neuroimaging findings indicate resolution of the restricted diffusion in the myelinated white matter (86). This suggests that the myelination itself is not delayed and is probably due to coalescence of the myelin vacuoles. Fractional anisotropy values in the myelinated white matter have been reported to be normal initially and subsequently decrease, indicating axonal loss (86). With nonketotic hyperglycinemia, ^{1}H MR spectroscopy will reveal a striking increase in the glycine peak level at 3.55 ppm (Fig 12c) (87,88). Because the glycine peak cannot be distinguished from the normal myo-inositol peak on short-echo MR spectra, the elevation in glycine concentration might be best evaluated by using long-echo ^{1}H MR spectra. With measurement of glycine concentrations, ^{1}H MR spectroscopic findings may not only suggest the diagnosis of nonketotic hyperglycinemia but also be used to monitor the effects of therapeutic interventions.

Homocystinuria

Homocysteine is a key product in the catabolism pathway of methionine. Homocystinuria may be caused by the malfunction of three enzymes: cystathionine β-synthase, methionine synthase, and methylene tetrahydrofolate reductase.

CBSD: OMIM 236200.—CBSD, or classic homocystinuria, is an autosomal recessive disorder that results in impaired synthesis of cystathionine and abnormal accumulation of homocysteine, methionine, and other metabolites (89). The estimated incidence is approximately one to nine in 100 000 individuals.

CBSD is a multisystem disease characterized by intellectual disability, lens dislocations and mal-

Figure 12. Nonketotic hyperglycinemia in a 5-day-old neonate who presented with severe seizures. **(a)** Axial T2-weighted MR image shows diffuse swelling and high signal intensity of the white matter. **(b)** Coronal ADC map reveals areas of low ADC value (arrow) in the corticospinal tracts, representing restricted diffusion. In addition, the "bull's head" appearance of the ventricular system suggests agenesis or severe hypogenesis of the corpus callosum. **(c)** Short echo time (echo time, 32 msec) water-suppressed ^{1}H MR spectra from the basal ganglia show an elevated glycine peak level (arrow) at 3.55 ppm. (Reprinted, with permission, from reference 11.)

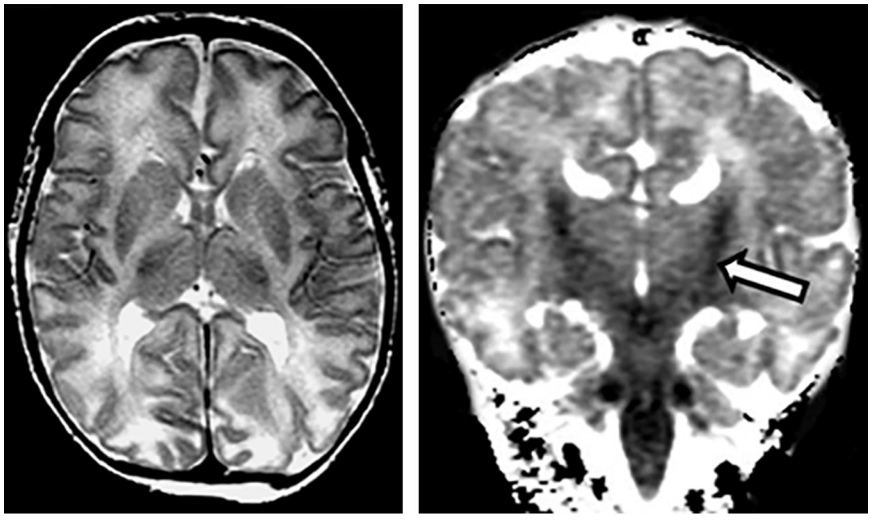

a. **b.**

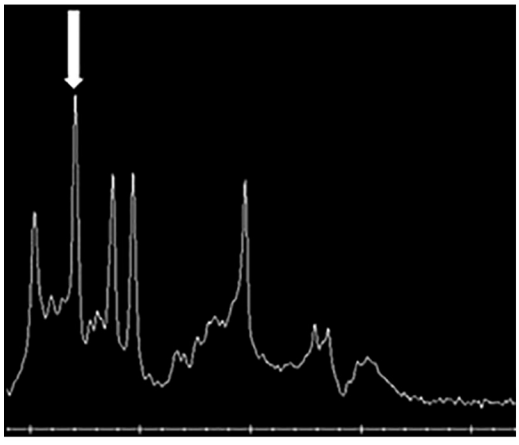

c.

formations, occlusive vascular events, and skeletal deformities (89). Intellectual disability is the most common neurologic manifestation; however, the spectrum of cognitive function ranges from normal cognitive function to profound intellectual disability. In addition, psychiatric problems, seizures, and/or extrapyramidal signs may be present. Thromboembolic events secondary to hypercoagulability are an important cause of morbidity and mortality, and they may cause occlusive peripheral venous and arterial diseases, cerebrovascular events, and myocardial infarction.

The neuroimaging findings of CBSD include multiple cortical-subcortical infarctions of different ages in the cerebral and cerebellar hemispheres (90). Venous infarction may be seen secondary to dural sinus thrombosis (91). Diffuse white matter signal intensity changes also may be observed and suggest demyelination (92). MR angiography and MR venography may be helpful in detecting occlusive disease of large cerebral arteries and intracranial dural sinuses. In addition, T2-weighted MR images may show lens dislocation in the form of an abnormal position of the hypointense lens within a hyperintense vitreous chamber. If seen, this feature is highly suggestive of CBSD.

MTHFRD: OMIM 236250.—MTHFRD is an autosomal recessive disorder that is caused by mutations in the *MTHFR* gene. This disorder is characterized by abnormal intracellular folic acid metabolism, which results in methyltetrahydrofolate deficiency and consequently homocystinuria and hypomethioninemia (93). The clinical manifestations vary with enzyme function and include developmental delay, motor and gait abnormalities, seizures, and psychiatric disorders (93).

In children who have MTHFRD, neuroimaging reveals abnormalities of the cerebral white matter that may be multifocal or diffuse; involve particularly the corpus callosum, external and extreme capsules, and anterior limb of the internal capsule; and may represent demyelination (94). The globi pallidi may have abnormal T2 signal intensity. Areas of vascular infarction are usually seen and have restricted diffusion during the acute phase. A decreased NAA peak level at ^{1}H MR spectroscopy has been reported (95).

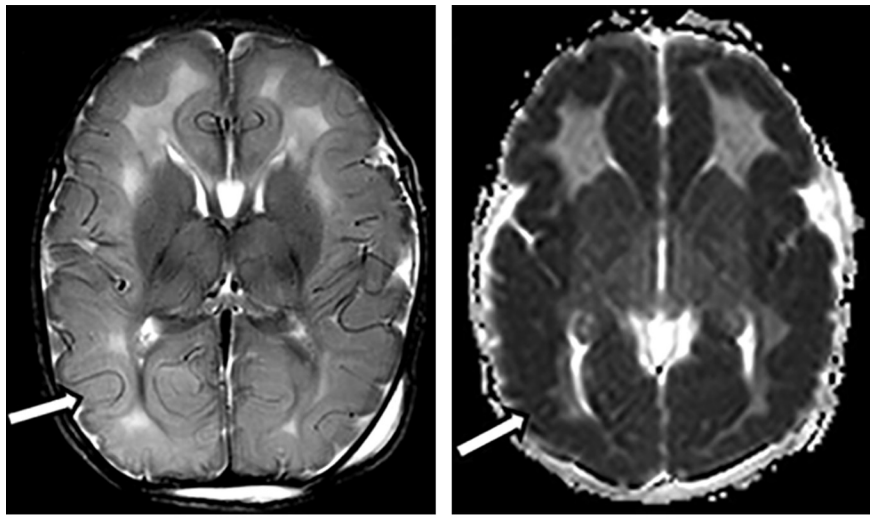

Figure 13. Molybdenum cofactor deficiency in a 4-day-old neonate who presented with severe seizures. **(a)** Axial T2-weighted MR image shows swollen gyri and diffusely increased signal intensity of the cortex, white matter, and deep gray matter structures. There is loss of sulci due to gyral swelling (arrow). **(b)** Axial ADC map shows areas of low ADC value (arrow), indicating restricted diffusion of the entire cerebral cortex. (Reprinted, with permission, from reference 11.)

Sulfite Oxidase Deficiency

Sulfite oxidase deficiency can occur in isolation (OMIM 272300)—in about 25% of cases—or in association with xanthine dehydrogenase deficiency as part of molybdenum cofactor deficiency (OMIM 252150) (96,97). Sulfite oxidase is located in the mitochondrial intermembranous space and is involved in the transfer of electrons from sulfites into the electron transport chain.

Sulfite oxidase deficiency and molybdenum cofactor deficiency manifest during the first days of life, with seizures, feeding difficulties, and vomiting. Facial dysmorphism may be present, and ectopia lentis can appear later.

MR images initially show extensive bilateral abnormal signal intensity, suggesting edema of the gray and white matter with cytotoxic edema (Fig 13) (98–100). The frontal and temporal cortices and the thalami may be spared. At early follow-up, the edema is decreased and curvilinear areas of reduced signal intensity appear at the gray matter–white matter junction, suggesting hemorrhagic deposits and laminar necrosis (98).

The final stage of sulfite oxidase deficiency is characterized by rapid development of extensive cystic leukomalacia, which may collapse (98–100). In addition, the cortex is globally atrophic, and areas of abnormal signal intensity are present bilaterally in the basal ganglia, internal capsule, and centrum semiovale. The cerebellum may be hypoplastic. ^{1}H MR spectroscopy reveals increased lactate and choline levels, elevated glutamine and glutamate levels (due to the inhibition of glutamate dehydrogenase by sulfites), and a reduced NAA level, as well as elevated peaks in the levels of several other metabolites that may have accumulated, including taurine at 3.42 and 3.24 ppm, *S*-sulfocysteine at 3.61 ppm, and cysteine at 2.92 and 2.97 ppm (99,100).

The clinical and neuroimaging findings of sulfite oxidase deficiency and hypoxic-ischemic injury are similar, so it is not surprising that most cases of sulfite oxidase deficiency are initially misdiagnosed as hypoxic-ischemic injury (97). However, there are important differences: Newborns with hypoxic-ischemic injury usually stabilize 1–2 weeks after they are born, whereas those with sulfite oxidase deficiency do not show improvement or stability. With hypoxic-ischemic injury, the caudate nucleus is rarely affected, whereas with sulfite oxidase deficiency, it is always involved (99). In patients with sulfite oxidase deficiency, as compared with those who have hypoxic-ischemic injury, the peak choline level at ^{1}H MR spectroscopy is increased rather than reduced (100).

Conclusion

Organic acidemias and aminoacidopathies include a variety of inborn errors of metabolism that are caused by defects in intermediary metabolic pathways of carbohydrates, amino acids, and fatty acid oxidation. These defects lead to the accumulation of organic acids and amino acids in body tissues and organs, including the brain. Several organic acidemias and aminoacidopathies manifest as acute encephalopathy during the neonatal–early infantile period. Although metabolic and/or genetic laboratory tests are needed to confirm the diagnosis, the results of careful pattern recognition at neuroimaging (Table 3)—especially with integration of conventional and advanced MR imaging techniques—may suggest the diagnosis and help guide management. Imaging findings also help to distinguish organic acidemias and aminoacidopathies from more common disorders with similar clinical manifestations. Furthermore, advanced neuroimaging techniques can be used to clarify

Table 3: Brain Regions Involved with Pediatric Organic Acidemias and Aminoacidopathies

Disease	Cortex	Basal Ganglia	White Matter	Corpus Callosum	Cerebellum	Brainstem
Propionic acidemia	+	+	+	-	+	+
MMA	-	+	+	-	-	-
Isovaleric acidemia	-	+	-	-	-	-
MCCD	-	-	+	-	+	+
Biotinidase deficiency	+	-	+	-	-	-
HSD	-	-	-	-	-	-
βKD	-	+	-	-	+	-
Canavan disease	-	+	+	-	+	+
GA1	-	+	+	-	+	-
L2HGA	-	+	+	+	+	-
D2HGA	+	+	+	-	-	-
5-Oxoprolinuria	+	-	-	-	-	-
3HBA	+	-	-	+	+	-
3HMGD	-	-	+	-	+	+
Phenylketonuria	-	+	+	-	-	-
TYRSN1	-	+	-	-	-	-
MSUD	-	+	+	-	+	+
NKH	-	-	+	Dysgenesis	+	-
CBSD	+	-	+	-	+	-
MTHFRD	-	+	+	-	+	+
SOD and MOCD	-	+	+	-	+	-

Note.—The brain regions involved with various pediatric organic acidemias and aminoacidopathies are categorized by using the neuroimaging-based pattern recognition approach to diagnosing and managing disease. + indicates that the metabolic disorder involves the given brain region. − indicates that the metabolic disorder does not involve the given brain region.
*βKD = β-ketothiolase deficiency, HSD = holocarboxylase synthetase deficiency, MMA = methylmalonic acidemia, NKH = nonketotic hyperglycinemia, PA = propionic acidemia, PKU = phenylketonuria, SOD = sulfite oxidase deficiency, TYRSN1 = tyrosinemia type 1.

disease mechanisms and, in cases of selected disorders, have the potential to serve as biomarkers for monitoring therapy response.

Acknowledgment.—The authors dedicate this article to the memory and legacy of their friend and colleague, Dr. Andrea Poretti, who passed away in March 2017.

References

1. Saudubray JM, Sedel F, Walter JH. Clinical approach to treatable inborn metabolic diseases: an introduction. J Inherit Metab Dis 2006;29(2-3):261–274.
2. Leonard JV, Morris AA. Diagnosis and early management of inborn errors of metabolism presenting around the time of birth. Acta Paediatr 2006;95(1):6–14.
3. Leijser LM, de Vries LS, Rutherford MA, et al. Cranial ultrasound in metabolic disorders presenting in the neonatal period: characteristic features and comparison with MR imaging. AJNR Am J Neuroradiol 2007;28(7):1223–1231.
4. Patay Z, Blaser SI, Poretti A, Huisman TA. Neurometabolic diseases of childhood. Pediatr Radiol 2015;45(suppl 3):S473–S484.
5. Patay Z. Diffusion-weighted MR imaging in leukodystrophies. Eur Radiol 2005;15(11):2284–2303.
6. Xu D, Bonifacio SL, Charlton NN, et al. MR spectroscopy of normative premature newborns. J Magn Reson Imaging 2011;33(2):306–311.
7. Bosemani T, Poretti A, Huisman TA. Susceptibility-weighted imaging in pediatric neuroimaging. J Magn Reson Imaging 2014;40(3):530–544.
8. Ozand PT, Gascon GG. Organic acidurias: a review—part 1. J Child Neurol 1991;6(3):196–219.
9. Baumgartner MR, Hörster F, Dionisi-Vici C, et al. Proposed guidelines for the diagnosis and management of methylmalonic and propionic acidemia. Orphanet J Rare Dis 2014;9:130.
10. Grünert SC, Müllerleile S, De Silva L, et al. Propionic acidemia: clinical course and outcome in 55 pediatric and adolescent patients. Orphanet J Rare Dis 2013;8:6.
11. Poretti A, Blaser SI, Lequin MH, et al. Neonatal neuroimaging findings in inborn errors of metabolism. J Magn Reson Imaging 2013;37(2):294–312.
12. Kandel A, Amatya SK, Yeh EA. Reversible diffusion weighted imaging changes in propionic acidemia. J Child Neurol 2013;28(1):128–131.
13. Cakir B, Teksam M, Kosehan D, Akin K, Koktener A. Inborn errors of metabolism presenting in childhood. J Neuroimaging 2011;21(2):e117–e133.
14. Karall D, Haberlandt E, Schimmel M, et al. Cytotoxic not vasogenic edema is the cause for stroke-like episodes in propionic acidemia. Neuropediatrics 2011;42(5):210.
15. Chemelli AP, Schocke M, Sperl W, Trieb T, Aichner F, Felber S. Magnetic resonance spectroscopy (MRS) in five patients with treated propionic acidemia. J Magn Reson Imaging 2000;11(6):596–600.
16. Davison JE, Davies NP, Wilson M, et al. MR spectroscopy-based brain metabolite profiling in propionic acidaemia: metabolic changes in the basal ganglia during acute decompensation and effect of liver transplantation. Orphanet J Rare Dis 2011;6:19.
17. Dave P, Curless RG, Steinman L. Cerebellar hemorrhage complicating methylmalonic and propionic acidemia. Arch Neurol 1984;41(12):1293–1296.
18. Lee NC, Chien YH, Peng SF, et al. Brain damage by mild metabolic derangements in methylmalonic acidemia. Pediatr Neurol 2008;39(5):325–329.

19. Radmanesh A, Zaman T, Ghanaati H, Molaei S, Robertson RL, Zamani AA. Methylmalonic acidemia: brain imaging findings in 52 children and a review of the literature. Pediatr Radiol 2008;38(10):1054–1061.
20. Vockley J, Ensenauer R. Isovaleric acidemia: new aspects of genetic and phenotypic heterogeneity. Am J Med Genet C Semin Med Genet 2006;142C(2):95–103.
21. Moorthie S, Cameron L, Sagoo GS, Bonham JR, Burton H. Systematic review and meta-analysis to estimate the birth prevalence of five inherited metabolic diseases. J Inherit Metab Dis 2014;37(6):889–898.
22. Sogut A, Acun C, Aydin K, Tomac N, Demirel F, Aktuglu C. Isovaleric acidaemia: cranial CT and MRI findings. Pediatr Radiol 2004;34(2):160–162.
23. Baumgartner MR, Almashanu S, Suormala T, et al. The molecular basis of human 3-methylcrotonyl-CoA carboxylase deficiency. J Clin Invest 2001;107(4):495–504.
24. Grünert SC, Stucki M, Morscher RJ, et al. 3-methylcrotonyl-CoA carboxylase deficiency: clinical, biochemical, enzymatic and molecular studies in 88 individuals. Orphanet J Rare Dis 2012;7:31.
25. Alshumrani GA, Patay Z. Brain magnetic resonance imaging and proton MR spectroscopic findings after metabolic crisis in 3-methylcrotonylglycinuria. Ann Saudi Med 2015;35(1):64–68.
26. de Kremer RD, Latini A, Suormala T, et al. Leukodystrophy and CSF purine abnormalities associated with isolated 3-methylcrotonyl-CoA carboxylase deficiency. Metab Brain Dis 2002;17(1):13–18.
27. Wolf B. The neurology of biotinidase deficiency. Mol Genet Metab 2011;104(1-2):27–34.
28. Desai S, Ganesan K, Hegde A. Biotinidase deficiency: a reversible metabolic encephalopathyn—neuroimaging and MR spectroscopic findings in a series of four patients. Pediatr Radiol 2008;38(8):848–856.
29. Bhat MD, Bindu PS, Christopher R, Prasad C, Verma A. Novel imaging findings in two cases of biotinidase deficiency: a treatable metabolic disorder. Metab Brain Dis 2015;30(5):1291–1294.
30. Mc Sweeney N, Grunewald S, Bhate S, Ganesan V, Chong WK, Hemingway C. Two unusual clinical and radiological presentations of biotinidase deficiency. Eur J Paediatr Neurol 2010;14(6):535–538.
31. Wolf B. Biotinidase deficiency should be considered in individuals exhibiting myelopathy with or without and vision loss. Mol Genet Metab 2015;116(3):113–118.
32. Donti TR, Blackburn PR, Atwal PS. Holocarboxylase synthetase deficiency pre and post newborn screening. Mol Genet Metab Rep 2016;7:40–44.
33. Squires L, Betz B, Umfleet J, Kelley R. Resolution of subependymal cysts in neonatal holocarboxylase synthetase deficiency. Dev Med Child Neurol 1997;39(4):267–269.
34. Bandaralage SP, Farnaghi S, Dulhunty JM, Kothari A. Antenatal and postnatal radiologic diagnosis of holocarboxylase synthetase deficiency: a systematic review. Pediatr Radiol 2016;46(3):357–364.
35. Fukao T, Scriver CR, Kondo N; t2 Collaborative Working Group. The clinical phenotype and outcome of mitochondrial acetoacetyl-CoA thiolase deficiency (beta-ketothiolase or T2 deficiency) in 26 enzymatically proved and mutation-defined patients. Mol Genet Metab 2001;72(2):109–114.
36. Ozand PT, Rashed M, Gascon GG, et al. 3-Ketothiolase deficiency: a review and four new patients with neurologic symptoms. Brain Dev 1994;16(suppl):38–45.
37. O'Neill ML, Kuo F, Saigal G. MRI of pallidal involvement in beta-ketothiolase deficiency. J Neuroimaging 2014;24(4):414–417.
38. Patay Z. Metabolic disorders. In: Tortori-Donati P, ed. Pediatric neuroradiology: brain. Berlin, Germany: Springer, 2005; 543–721.
39. Kumar S, Mattan NS, de Vellis J. Canavan disease: a white matter disorder. Ment Retard Dev Disabil Res Rev 2006;12(2):157–165.
40. Brismar J, Brismar G, Gascon G, Ozand P. Canavan disease: CT and MR imaging of the brain. AJNR Am J Neuroradiol 1990;11(4):805–810.
41. Nguyen HV, Ishak GE. Canavan disease: unusual imaging features in a child with mild clinical presentation. Pediatr Radiol 2015;45(3):457–460.
42. Srikanth SG, Chandrashekar HS, Nagarajan K, Jayakumar PN. Restricted diffusion in Canavan disease. Childs Nerv Syst 2007;23(4):465–468.
43. Boy N, Mühlhausen C, Maier EM, et al. Proposed recommendations for diagnosing and managing individuals with glutaric aciduria type I: second revision. J Inherit Metab Dis 2017;40(1):75–101.
44. Kölker S, Koeller DM, Okun JG, Hoffmann GF. Pathomechanisms of neurodegeneration in glutaryl-CoA dehydrogenase deficiency. Ann Neurol 2004;55(1):7–12.
45. Garbade SF, Greenberg CR, Demirkol M, et al. Unravelling the complex MRI pattern in glutaric aciduria type I using statistical models: a cohort study in 180 patients. J Inherit Metab Dis 2014;37(5):763–773.
46. Mohammad SA, Abdelkhalek HS, Ahmed KA, Zaki OK. Glutaric aciduria type 1: neuroimaging features with clinical correlation. Pediatr Radiol 2015;45(11):1696–1705.
47. Van Schaftingen E, Rzem R, Veiga-da-Cunha M. L: -2-hydroxyglutaric aciduria, a disorder of metabolite repair. J Inherit Metab Dis 2009;32(2):135–142.
48. Patay Z, Mills JC, Löbel U, Lambert A, Sablauer A, Ellison DW. Cerebral neoplasms in L-2 hydroxyglutaric aciduria: 3 new cases and meta-analysis of literature data. AJNR Am J Neuroradiol 2012;33(5):940–943.
49. Moroni I, D'Incerti L, Farina L, Rimoldi M, Uziel G. Clinical, biochemical and neuroradiological findings in L-2-hydroxyglutaric aciduria. Neurol Sci 2000;21(2):103–108.
50. Steenweg ME, Salomons GS, Yapici Z, et al. L-2-hydroxyglutaric aciduria: pattern of MR imaging abnormalities in 56 patients. Radiology 2009;251(3):856–865.
51. Aydin K, Ozmen M, Tatli B, Sencer S. Single-voxel MR spectroscopy and diffusion-weighted MRI in two patients with l-2-hydroxyglutaric aciduria. Pediatr Radiol 2003;33(12):872–876.
52. Struys EA. D-2-hydroxyglutaric aciduria: unravelling the biochemical pathway and the genetic defect. J Inherit Metab Dis 2006;29(1):21–29.
53. van der Knaap MS, Jakobs C, Hoffmann GF, et al. D-2-hydroxyglutaric aciduria: further clinical delineation. J Inherit Metab Dis 1999;22(4):404–413.
54. Kwong KL, Mak T, Fong CM, Poon KH, Wong SN, So KT. D-2-hydroxyglutaric aciduria and subdural haemorrhage. Acta Paediatr 2002;91(6):716–718.
55. Eeg-Olofsson O, Zhang WW, Olsson Y, Jagell S, Hagenfeldt L. D-2-hydroxyglutaric aciduria with cerebral, vascular, and muscular abnormalities in a 14-year-old boy. J Child Neurol 2000;15(7):488–492.
56. Ristoff E, Mayatepek E, Larsson A. Long-term clinical outcome in patients with glutathione synthetase deficiency. J Pediatr 2001;139(1):79–84.
57. Al-Jishi E, Meyer BF, Rashed MS, et al. Clinical, biochemical, and molecular characterization of patients with glutathione synthetase deficiency. Clin Genet 1999;55(6):444–449.
58. Li X, Ding Y, Liu Y, et al. Five Chinese patients with 5-oxoprolinuria due to glutathione synthetase and 5-oxoprolinase deficiencies. Brain Dev 2015;37(10):952–959.
59. Loupatty FJ, van der Steen A, Ijlst L, et al. Clinical, biochemical, and molecular findings in three patients with 3-hydroxyisobutyric aciduria. Mol Genet Metab 2006;87(3):243–248.
60. Sasaki M, Yamada N, Fukumizu M, Sugai K. Basal ganglia lesions in a patient with 3-hydroxyisobutyric aciduria. Brain Dev 2006;28(9):600–603.
61. Sasaki M, Kimura M, Sugai K, Hashimoto T, Yamaguchi S. 3-Hydroxyisobutyric aciduria in two brothers. Pediatr Neurol 1998;18(3):253–255.
62. Chitayat D, Meagher-Villemure K, Mamer OA, et al. Brain dysgenesis and congenital intracerebral calcification associated with 3-hydroxyisobutyric aciduria. J Pediatr 1992;121(1):86–89.
63. Fukao T, Mitchell G, Sass JO, Hori T, Orii K, Aoyama Y. Ketone body metabolism and its defects. J Inherit Metab Dis 2014;37(4):541–551.

64. van der Knaap MS, Bakker HD, Valk J. MR imaging and proton spectroscopy in 3-hydroxy-3-methylglutaryl coenzyme A lyase deficiency. AJNR Am J Neuroradiol 1998;19(2):378–382.
65. Yalçinkaya C, Dinçer A, Gündüz E, Fiçicioğlu C, Koçer N, Aydin A. MRI and MRS in HMG-CoA lyase deficiency. Pediatr Neurol 1999;20(5):375–380.
66. Hoffmann GF, Kölker S. Defects in amino acid catabolism and the urea cycle. Handb Clin Neurol 2013;113:1755–1773.
67. Blau N, van Spronsen FJ, Levy HL. Phenylketonuria. Lancet 2010;376(9750):1417–1427.
68. Blau N, Hennermann JB, Langenbeck U, Lichter-Konecki U. Diagnosis, classification, and genetics of phenylketonuria and tetrahydrobiopterin (BH4) deficiencies. Mol Genet Metab 2011;104(suppl):S2–S9.
69. Anderson PJ, Leuzzi V. White matter pathology in phenylketonuria. Mol Genet Metab 2010;99(suppl 1):S3–S9.
70. Hood A, Antenor-Dorsey JA, Rutlin J, et al. Prolonged exposure to high and variable phenylalanine levels over the lifetime predicts brain white matter integrity in children with phenylketonuria. Mol Genet Metab 2015;114(1):19–24.
71. Mastrangelo M, Chiarotti F, Berillo L, et al. The outcome of white matter abnormalities in early treated phenylketonuric patients: a retrospective longitudinal long-term study. Mol Genet Metab 2015;116(3):171–177.
72. de Laet C, Dionisi-Vici C, Leonard JV, et al. Recommendations for the management of tyrosinaemia type 1. Orphanet J Rare Dis 2013;8:8.
73. Sener RN. Brain magnetic resonance imaging in tyrosinemia. Acta Radiol 2005;46(6):618–620.
74. Sener RN. Tyrosinemia: computed tomography, magnetic resonance imaging, diffusion magnetic resonance imaging, and proton spectroscopy findings in the brain. J Comput Assist Tomogr 2005;29(3):323–325.
75. Schadewaldt P, Wendel U. Metabolism of branched-chain amino acids in maple syrup urine disease. Eur J Pediatr 1997;156(suppl 1):S62–S66.
76. Morton DH, Strauss KA, Robinson DL, Puffenberger EG, Kelley RI. Diagnosis and treatment of maple syrup disease: a study of 36 patients. Pediatrics 2002;109(6):999–1008.
77. Simon E, Fingerhut R, Baumkötter J, Konstantopoulou V, Ratschmann R, Wendel U. Maple syrup urine disease: favourable effect of early diagnosis by newborn screening on the neonatal course of the disease. J Inherit Metab Dis 2006;29(4):532–537.
78. Jan W, Zimmerman RA, Wang ZJ, Berry GT, Kaplan PB, Kaye EM. MR diffusion imaging and MR spectroscopy of maple syrup urine disease during acute metabolic decompensation. Neuroradiology 2003;45(6):393–399.
79. Ha JS, Kim TK, Eun BL, et al. Maple syrup urine disease encephalopathy: a follow-up study in the acute stage using diffusion-weighted MRI. Pediatr Radiol 2004;34(2):163–166.
80. Righini A, Ramenghi LA, Parini R, Triulzi F, Mosca F. Water apparent diffusion coefficient and T2 changes in the acute stage of maple syrup urine disease: evidence of intramyelinic and vasogenic-interstitial edema. J Neuroimaging 2003;13(2):162–165.
81. Parmar H, Sitoh YY, Ho L. Maple syrup urine disease: diffusion-weighted and diffusion-tensor magnetic resonance imaging findings. J Comput Assist Tomogr 2004;28(1):93–97.
82. Applegarth DA, Toone JR. Glycine encephalopathy (nonketotic hyperglycinaemia): review and update. J Inherit Metab Dis 2004;27(3):417–422.
83. Suzuki Y, Kure S, Oota M, Hino H, Fukuda M. Nonketotic hyperglycinemia: proposal of a diagnostic and treatment strategy. Pediatr Neurol 2010;43(3):221–224.
84. Shah DK, Tingay DG, Fink AM, Hunt RW, Dargaville PA. Magnetic resonance imaging in neonatal nonketotic hyperglycinemia. Pediatr Neurol 2005;33(1):50–52.
85. Khong PL, Lam BC, Chung BH, Wong KY, Ooi GC. Diffusion-weighted MR imaging in neonatal nonketotic hyperglycinemia. AJNR Am J Neuroradiol 2003;24(6):1181–1183.
86. Mourmans J, Majoie CB, Barth PG, Duran M, Akkerman EM, Poll-The BT. Sequential MR imaging changes in nonketotic hyperglycinemia. AJNR Am J Neuroradiol 2006;27(1):208–211.
87. Huisman TA, Thiel T, Steinmann B, Zeilinger G, Martin E. Proton magnetic resonance spectroscopy of the brain of a neonate with nonketotic hyperglycinemia: in vivo-in vitro (ex vivo) correlation. Eur Radiol 2002;12(4):858–861.
88. Viola A, Chabrol B, Nicoli F, Confort-Gouny S, Viout P, Cozzone PJ. Magnetic resonance spectroscopy study of glycine pathways in nonketotic hyperglycinemia. Pediatr Res 2002;52(2):292–300.
89. Morris AA, Kožich V, Santra S, et al. Guidelines for the diagnosis and management of cystathionine beta-synthase deficiency. J Inherit Metab Dis 2017;40(1):49–74.
90. Ruano MM, Castillo M, Thompson JE. MR imaging in a patient with homocystinuria. AJR Am J Roentgenol 1998;171(4):1147–1149.
91. Buoni S, Molinelli M, Mariottini A, et al. Homocystinuria with transverse sinus thrombosis. J Child Neurol 2001;16(9):688–690.
92. Brenton JN, Matsumoto JA, Rust RS, Wilson WG. White matter changes in an untreated, newly diagnosed case of classical homocystinuria. J Child Neurol 2014;29(1):88–92.
93. Huemer M, Mulder-Bleile R, Burda P, et al. Clinical pattern, mutations and in vitro residual activity in 33 patients with severe 5, 10 methylenetetrahydrofolate reductase (MTHFR) deficiency. J Inherit Metab Dis 2016;39(1):115–124.
94. van den Berg M, van der Knaap MS, Boers GH, Stehouwer CD, Rauwerda JA, Valk J. Hyperhomocysteinaemia; with reference to its neuroradiological aspects. Neuroradiology 1995;37(5):403–411.
95. Engelbrecht V, Rassek M, Huismann J, Wendel U. MR and proton MR spectroscopy of the brain in hyperhomocysteinemia caused by methylenetetrahydrofolate reductase deficiency. AJNR Am J Neuroradiol 1997;18(3):536–539.
96. Brown GK, Scholem RD, Croll HB, Wraith JE, McGill JJ. Sulfite oxidase deficiency: clinical, neuroradiologic, and biochemical features in two new patients. Neurology 1989;39(2 Pt 1):252–257.
97. Sass JO, Gunduz A, Araujo Rodrigues Funayama C, et al. Functional deficiencies of sulfite oxidase: differential diagnoses in neonates presenting with intractable seizures and cystic encephalomalacia. Brain Dev 2010;32(7):544–549.
98. Dublin AB, Hald JK, Wootton-Gorges SL. Isolated sulfite oxidase deficiency: MR imaging features. AJNR Am J Neuroradiol 2002;23(3):484–485.
99. Eichler F, Tan WH, Shih VE, Grant PE, Krishnamoorthy K. Proton magnetic resonance spectroscopy and diffusion-weighted imaging in isolated sulfite oxidase deficiency. J Child Neurol 2006;21(9):801–805.
100. Hoffmann C, Ben-Zeev B, Anikster Y, et al. Magnetic resonance imaging and magnetic resonance spectroscopy in isolated sulfite oxidase deficiency. J Child Neurol 2007;22(10):1214–1221.